Spring 2016

Land Use And Land Cover Classification And Change Detection Using Naip Imagery From 2009 To 2014: Table Rock Lake Region, Missouri

Dexuan Sha Sha

LAND USE AND LAND COVER CLASSIFICATION AND CHANGE DETECTION USING NAIP IMAGERY FROM 2009 TO 2014: TABLE ROCK LAKE REGION, MISSOURI

A Masters Thesis

Presented to

The Graduate College of

Missouri State University

In Partial Fulfillment

Of the Requirements for the Degree

Master of Natural and Applied Science

By

Dexuan Sha

May 2016

LAND USE AND LAND COVER CLASSIFICATION AND CHANGE DETECTION USING NAIP IMAGERY FROM 2009 TO 2014: TABLE ROCK LAKE REGION, MISSOURI

Geography, Geology and Planning

Missouri State University, May 2016

Master of Natural and Applied Science

Dexuan Sha

ABSTRACT

Land use and land cover (LULC) of Table Rock Lake (TRL) region has changed over the last half century after the construction of Table Rock Dam in 1959. This study uses one meter spatial resolution imagery to classify and detect the change of LULC of three typical waterside TRL regions. The main objectives are to provide an efficient and reliable classification workflow for regional level NAIP aerial imagery and identify the dynamic patterns for study areas. Seven class types are extracted by optimal classification results from year 2009, 2010, 2012 and 2014 of Table Rock Village, Kimberling City and Indian Point. Pixel-based post-classification comparison generated "from-to" confusion matrices showing the detailed change patterns. I conclude that object-based random trees achieve the highest overall accuracy and kappa value, compared with the other six classification approaches, and is efficient to make a LULC classification map. Major change patterns are that vegetation, including trees and grass, increased during the last five years period while residential extension and urbanization process is not obvious to indicate high economic development in the TRL region. By adding auxiliary spatial information and object-based post-classification techniques, an improved classification procedure can be utilized for LULC change detection projects at the region level.

KEYWORDS: object-based, land use and land cover, NAIP, random tree, Table Rock Lake

This abstract is approved as to form and content

_____

Dr. Xiaomin Qiu
Chairperson, Advisory Committee
Missouri State University

LAND USE AND LAND COVER CLASSIFICATION AND CHANGE DETECTION USING NAIP IMAGERY FROM 2009 TO 2014: TABLE ROCK LAKE REGION, MISSOURI

By

Dexuan Sha

A Masters Thesis
Submitted to the Graduate College
Of Missouri State University
In Partial Fulfillment of the Requirements
For the Degree of Master of Natural and Applied Science

May 2016

Approved:

_____
Dr. Xiaomin Qiu

_____
Dr. Xin Miao

_____
Dr. Songfeng Zheng

_____
Julie Masterson, PhD: Dean, Graduate College

ACKNOWLEDGEMENTS

First of all, I would like to thank my parents and friends for their consistent and unlimited support and encouragement.

Then I would like to acknowledge the following people in my thesis committee for their support during the course of my graduate studies. My advisor, Dr. Xiaomin Qiu, assisted me to find my research topic and define the final study sites with her professional and scientific experiences. Dr. Qiu also provided me and helped me greatly in research data collection from MSDIS. Sincere appreciation goes to Dr. Miao Xin who leads me to Remote sensing field with his enthusiasm and kindness. During the two year research and study, I learned scientific critical thinking, specialized knowledge from Dr. Miao's lectures, projects and literatures. I would also thank Dr. Zheng Songfeng, who first introduced applied mathematical application in pattern cognition field. I appreciate for their insightful and inspiring advices.

Also great appreciation for Laura and Jennifer, my friendly and warm heart colleagues, patiently answered my technological questions and shared their information and experiences.

Finally I would thank to whole Geography, Geology and Planning department, providing graduate teaching assistant opportunity that helps me to understand how daily school members work and also solves my financial issues.

TABLE OF CONTENTS

LIST OF TABLES

LIST OF FIGURES

INTRODUCTION

Land use and land cover (LULC) may reflect the complex land utilization and distribution of natural materials at global scale or regional scale. LULC change is important for understanding relationships and interactions between human behaviors and natural phenomena in order to develop policies corresponding to certain principles and social objectives. Although LULC changes can be monitored by traditional geographical survey, remote sensing techniques and methods are becoming widely adopted nowadays due to the capability of acquiring up-to-date information over large areas relatively cheap and fast.

There are various methods of classifying remote sensing data for determining LULC distribution and change at local level. Pre-classification and post-classification are two methods in opposite perspectives for change detection and classification (Yuan, Elvidge & Lunetta, 1998). Algebra-based detection, such as image differencing, image ratioing and change vector analysis approaches, and transformation-based detection, including principal component analysis, are two main pre-classification techniques. These methods could detect the change, but could not provide information presenting how each land type changes. On the contrary, post-classification comparison approaches use separate classifications of images acquired at multi-temporal points to generate different maps from which "from-to" change information can be produced. The accuracy of post-classification is highly dependent on the result of individual classification. Edge effects and registration errors can also cause possible errors in the classification process. With the increasing availability of very high resolution imagery, object-based

classification methods have been created for better accuracy compared with traditional pixel-based methods. Random trees, decision trees and nearest-neighbor classifier are typical machine learning techniques for classifying objects by using training samples collected from image interpretation or ground control points. The optimally accurate and efficient classification method may depend on the specific imagery. Object-based classification methods on NAIP imagery have been frequently utilized in vegetation or precision agriculture, land cover extraction, and urban planning fields, but there is no conclusion about which algorithm can generate the most accurate result efficiently.

Table Rock Lake is an artificial reservoir in the Ozarks of southwestern Missouri and northwestern Arkansas. The lake is impounded by Table Rock Dam, which was constructed by the U.S. Army Corps of Engineers on the White River in 1954-1958. Table Rock Lake region, especially Branson city, becomes one of the most popular destinations for vacationers from Missouri and neighboring areas. Table Rock State Park, Silver dollar city and several commercial marinas are located along the lake. Fishing and entertainment businesses are prosperous while new fish hatchery are being led by the local government. Under this potential background, how LULC distributes and changes in Table Rock region beside Branson city is a significant factor for local governor, land planner and industrial investor to make decisions. LULC research of Table Rock Lake watershed has been done in 1992 and 1995, but consistently recent study is absent. The pervious LULC classification is based on a larger scale of 30 meter resolution Landsat TM images which may lead to inaccurate classification. Local level classification and change detection based on one meter spatial resolution data for this area is imperatively required.

This study investigates the methods of object-based classifications and post-classification change detection of multi-temporal high resolution NAIP aerial imagery of the Table Rock Lake region for 2009, 2010, 2012 and 2014. The objectives of this research are: (1) to classify the LULC of Table Rock Region in the recent five years using high spatial resolution aerial photographs; (2) to extract the obvious dynamic change detection of typical Table Rock lakeside areas, especially in Table Rock Village, Kimberling City and Indian Point; (3) to create an efficient and reliable procedure to make a classification map based on NAIP imagery.

LITERATURE REVIEW

Land Use and Land Cover Change Detection

Land use and land cover change (LULCC) is an important field in global and regional environment change and sustainable development issue research. Change detection is the process of identifying differences in the state of an object or phenomenon by observing it at different times (Singh, 1989). Effective and efficient approach to extract dynamic change detection of land covers is extremely important for understanding relationships and interactions between human behavior and natural phenomena in order to promote better decision making.

Land use refers to various types of arrangement, activities and inputs human use in a landscape to achieve a specific purpose. Land cover refers to physical and environmental cover of land surface including waterbodies, vegetation (trees, bushes, fields and grass), bare ground, and impervious artificial constructions. Land use and land cover shows a similar definition of land surface type classes, while land use emphases dynamic situation influenced by factitious objective and land cover focuses on static features of natural formed environment.

LULCC researches vary from large to small scales based on their study objectives. Globally, Hansen, DeFries, Townshend, & Sohlberg (2000) produced a 1 km spatial resolution land cover classification using data for 1992 to 1993 from the advanced high resolution radiometer. Twelve classes are extracted globally, and vegetation class is focused. Depictions of forests and woodland are detected, which shows an agreement with other sources. Regionally, Xiuwan (2002) utilized Landsat TM data from year 1985,

1987, 1990 and 1993 of Ansan City, Korea and post-classification approach to obtain land cover change in Korean west coastal zone. Natural forces and human activities have impacted on the regional development. For more specific land type change detection, e.g. vegetation, Cohen, Yang, & Kennedy (2010) characterized vegetation change over large areas annually at the spatial grain of anthropogenic disturbance. Vegetation change tracker (VCT), an automated algorithm, was proposed for reconstructing forest disturbance history using Landsat time series stacks (Huang et al., 2010). Huang used a biennial temporal interval from 1984 to 2006 for over six validation sites to examine disturbance patterns of the forest areas.

Many LULCC techniques are developed and created to quantitatively analyze the multi-temporal datasets for the temporal effects. The dataset includes classical remote sensing data, such as Landsat Thematic Mapper (TM), Satellite Probatoired' Obsevation de la Terre (SPOT), Advanced Very High Resolution Radiometer (AVHRR), and new generation aerial photography, such as Digital Orthophoto Quarter Quads (DOQQs). Many change detection approaches have been reviewed and summarized (Singh, 1989; Lu, Mausel, Brondizio, & Moran, 2004). Time series analysis (TSA) involves methods of analyzing time series data in order to extract meaningful statistics and other characteristics. Most change detection studies analyze two temporal steps and may be understood as bi-temporal before/after analyses. Remote sensing based time series analyses of change detection were developed to overcome this limitation. This review mainly divides the change detection methods into six categories: (1) algebra, (2) transformation, (3) classification, (4) Advanced motels, (5) object-based change detection, and (6) other approach. The first five categories are reviewed as following.

Algebra Based Detection. The image algebra methods conduct change extraction based on spectral values, backscatter values, indices, texture features and related properties. They usually provide a changing confusion matrix, which is simple to understand and interpret.

Image differencing and image ratioing are two of the earliest change detection algorithms. Image differencing includes the subtraction of a date one image from a co-registered second date image. Image differencing is easy to apply and result interpretation is straightforward, but it requires threshold selection. Image ratioing calculates the ratio value of two co-registered images by band, which handles calibration errors better. However both methods cannot provide a detailed change matrix.

Change Vector Analysis (CVA) is a bi-temporal change detection method that calculates change direction from spectral vector, and then total change magnitude per pixel is computed in n-dimensional change space. The advantages of CVA method are its capability of using all spectral input information and the provision of directional information, which facilitates the interpretation of occurring changes. Chen, Gong, He, Pu, and Shi (2003) adopted an improved CVA on a case study of land-use change detection in the Haidian district of Beijing, China. Their CVA includes Double-Window flexible pace search (DFPS) method, which aims at determining the threshold of change magnitude efficiently, and the new change direction method combined a single image classification and a minimum-distance categorization based upon the cosine values of the change vector.

Vegetation index differencing methods produce vegetation index separately, then subtract the second-date vegetation index from the first-date vegetation index.

Normalized difference change detection (NDCD) is one of vegetation index differencing methods that utilized Normalized Difference Vegetation Index (NDVI) to extract vegetation change results. Gianinetto & Villa (2011) used the NDCD technique, and a case study of New Orleans showing the use of NDCD for flood mapping. They compared the NDCD to other standard change detection methods, such as near-infrared normalized difference, unsupervised post-classification comparison and CVA, on the potentialities and performances. This approach may emphasize differences in the spectral response of different features.

Transformation Based Change Detection. Transformation based methods include methods such as Principal Component Analysis (PCA), Iteratively-Reweighted Alteration Detection (IR-MAD) and Minimum Noise Fraction (MNF). Their advantages lie in reducing data redundancy between spectral bands and emphasizing different information in derived components. However, they cannot provide detailed change matrices, and require threshold selection to identify changed areas. Another disadvantage is the difficulty in interpreting and labelling the change information on transformed images.

PCA is a multivariate statistical analysis technique used to reduce the number of spectral components to fewer principle components that account for the most variance in the original high dimensional images (Ingebritsen & Lyon, 1985; Eklundh & Singh, 1993). PCA can reduce data redundancy between bands and emphasize different information in the derived components.

Byrne, Crapper, and Mayo (1980) studied the effectiveness of principal components analysis for the identification of land cover changes and mapping of bush

fires and subsequent vegetation regeneration, respectively. However, they did not provide any quantitative analysis of their results. Toll, Royal, and Davis (1980) reported that principal components transformation when used for urban change detection produced poor change detection results compared with simple image differencing of band 2 or 4 data. This technique is often used to reduce the dimensionality of change extraction results derived by other means. IR-MAD is a robust and automatic change extraction method and widely used for automatic radiometric normalization. Developed from the multivariate alteration detection (MAD), IR-MAD is designed to identify unchanged pixels which can subsequently be used to define a regression equation for the radiometric normalization of multispectral images (Nielsen & Conradsen, 1997).

Classification-Based Detection. The classification-based methods can identify the land use and land cover change. Post-classification comparison (PCC) is widely used on the separate classification of two or more images taken in a time series (Van Oort, 2007; Singh, 1989; Chen et al., 2003). PCC holds promise because data from two dates are separately classified, which thereby minimizes the problem of normalizing for atmospheric and sensor differences between two dates. After the image classification, the change matrix statistics are calculated and extracted to interpret different classes. The primary advantage of PCC is that it operates independently from input data. Also PCC minimizes the impacts of atmospheric, sensor and environmental differences between multi-temporal images and provides a complete change confusion matrix. Thus, classification results derived from SAR and optical data, or other data can be compared. No radiometric preprocessing or adjustment between images is required.

Advanced Models. This category includes spectral mixture models, fuzzy change detection and biophysical parameter estimation models. In these methods, the image reflectance values are often transformed to natural based parameters or formulas through linear or complex mathematical models. The converted parameters are more straightforward to interpret, and can extract specific land cover information better than unprocessed spectral bands. However, these methods are time-consuming, and have difficulty in establishing suitable models for the conversion of image reflectance values to biophysical and other advanced parameters. Multi-temporal spectral mixture analysis (SMA) is the most popular model created to detect land cover change, vegetation variation, fire and grading patterns, and urbanization process. SMA assumes that multispectral image pixels can be defined in terms of their subpixel proportions of pure spectral components which may then be related to surface constituents in a scene (Rashed Weeks, Stow, & Fugate, 2005).

Object-based Change Detection. Object-based change detection (OBCD) methods are becoming more and more popular since the wide availability of very high spatial resolution (VHSR) imagery. The arbitrary change detection of OBCD is based on image pixel which is considered not a true geographical object, and the image cell representing spectral values in a net gird lacks correspondence with real-world. OBIA allows the segmentation and extraction of features from VHSR data, and also facilitates the integration of raster-based processing and vector-based GIS.

OBCD includes direct object comparison (DOC) approach, classified objects comparison (COC) based approach, and multi-temporal object change detection. DOC between the image-objects from different time points is performed for change detection,

which is similar to pixel-based methods. However, geometrical features (area, length and compactness), spectral information (mean and standard deviation band values) and other extracted features are compared among the image objects. COC method allows creating confusion matrix indicting the "from-to" changes by comparing independently classified bi-temporal images with their extracted objects. There are different theoretical types of OBCD based on post-classification comparison. Stow (2010) argued that the same segmentation and classification algorithms with similar parameters, class schema and output format should be used.

Geographical Information System (GIS) Contribution. A GIS may be defined as a container of maps in digital form or a computerized tool for solving geographic problems. However, Longley, Goodchild, Maguire, and Rhind (2011) stated, "Everyone has a favorite definition of GIS, and there are many to choose from" (p. 35). In the LUCC field, GIS serves at least three important roles, such as data integrator, visualization and analysis platform. GIS techniques are powerful when multi-source data are utilized in change detection studies.

In the initial stage of applications, data can be either already available as ArcInfo coverages (statistical databases), or can be captured by scanning and digitizing (remote sensing images). A GIS can spatially integrate several variables, such as vegetation, topography, climatology, and the existing information with position characteristics. These variables can be created, transformed and combined in the GIS. GIS is a necessary tool in the model construction and calibration, and plays an essential role when the predictions are distributed and reproduced. The cellular automation predictions (or other prediction models) generated can be reintroduced into the GIS datasets available for application,

allowing decisions to be made with the data. The change detection techniques and analysis methods can be utilized in the GIS.

For different change detection method, Lu, Mausel, Brondizio, and Moran (2004) argued that post-classification comparison is much suitable with sufficient training samples available. With development of higher spatial resolution images, object-based change detection method can handle objects for different land use types, e.g. buildings and vehicles, with much accuracy and efficacy. Object-based methods may have more potential in LULCC detection.

Remote Sensing and GIS Techniques in Imagery Classification Workflow

Remote Sensing (RS) and Geographic Information Science (GIS) have proved to be strong tools in facilitating land use and land cover analysis. The common research processing workflow including image preprocessing, image enhancement, image classification and accuracy assessment can be easily executed in the RS and GIS environment.

Data Pre-processing. Image Pre-processing refers to image restoration and rectification, which is aimed at correcting the specific radiometric and geometric distortions of data. The data should represent similar atmospheric conditions which can be achieved by relative atmospheric conditions. However many change detection and classification techniques do not require absolute atmospheric correction. Image registration, segmentation and enhancement will be discussed in the following section.

Image registration is the process of transforming different sets of data into one coordinate system (Brown, 1992). Data may be multiple photographs, data from different

sensors, times, depths, or viewpoints. Multi-temporal image registration is an essential pre-processing technique for change detection, and ensures that the changes detected are not due to land surface objects compared at different geographic locations at one time or another (Townshend, Justice, Gurney, & McManus, 1992). The performance of image registration is typically related to two factors: image's spatial resolution and the structure of geographic objects of interest. For example, misregistration possibly occurs at the pixel level using high spatial resolution imagery (e.g., 1 m IKONOS), while it is easier to achieve registration accuracy at the sub pixel level using relatively low resolution data (e.g., 30 m Landsat). In addition to spatial resolution, Dai and Khorram (1998) have proven further that the finer the spatial frequency in the images, the greater the effects of misregistration on change detection accuracy. In their tests, the registration accuracy of less than one-fifth of a pixel was required in order to detect 90% of the true changes (Dai & Khorram, 1998).

Image Enhancement. Image enhancement plays an increasing crucial role in improving the quality and appearance of images. The main function of image enhancement is intuitionistic visual analysis and sequent machine analysis (Jensen, 2007).

Remote sensing indices, a kind of image enhancement, have been studied. Normalized Difference Vegetation Index (NDVI) (Fuller, 1998) and the Normalized Difference Water Index (NDWI) (Gao, 1996) are two examples of widely-used indices. Lunetta, Knight, Ediriwickrema, Lyon, & Worthy (2006) utilized the MODIS NDVI data and automated data processing techniques to represent an automated approach monitoring

annual land-cover change and vegetation condition for the Albemarle-Pamlico Estuary System (APES) region of the U.S.

Image Segmentation. Image segmentation is the process of partitioning an image into groups of pixels that are homogeneous and spatially adjacent by minimizing the within-object variability compared to the between-object variability. The goal of segmentation is to simplify and change the representation of an image into something that is more meaningful and easier to analyze (Desclée, Bogaert & Defourny, 2006).

Image segmentation is an important work procedure for the object-based classification and feature extraction of high resolution digital images. The segmentation result can affect subsequent processing. At present, the main image segmentation method is edge-based segmentation (Liu & Gao, 2008). Adopting the edge-based segmentation, the accuracy of edge positioning is high, whereas the consecutive edge composed of a serial of unique pixels cannot be produced. So a sequent process including the bulky detected edge points should be required.

Image Classification. Image classification methods are developed for passive remote sensing images aimed at generating land-cover maps. The supervised and unsupervised classification techniques are widely used, and they differ in how the classification is performed. In this section, not only are these two general techniques mentioned but also the new developed methods such as Semi-supervised Learning (SSL) and Active Learning (AL) classification.

Supervised Learning Classification. Supervised classification techniques require a set of labeled samples to train the classification algorithm. Statistical and machine learning methods attach the importance to the classification and analysis of multispectral

Remote Sensing (RS) data. The machine learning techniques, such as k-nearest neighbor classifier (Samaniego, Bárdossy, & Schulz, 2008), decision trees, maximum likelihood classifier (Rozenstein & Karnieli, 2011), genetic algorithms based classifiers (Bandyopadhyay & Pal, 2001), and ant colony algorithms (Liu, Li, Liu, & He, 2008) have been studied in the past.

Rozenstein and Karnieli (2011) compared several established methods for land-use classification using RS data, and found that using a combination of supervised and unsupervised training classes produced more accurate results than when using either of them separately in the northern Negev in Israel. Abd El-Kawy, Rød, Ismail, and Suliman (2001) applied the supervised classification method to four Landsat images collected over time (1984, 1999, 2005, and 2009) about recent and historical LULC conditions for the Western Nile Delta, and the results were further improved by employing image enhancement and visual interpretation. Hughes (1968) stated that the classification accuracy decreases by increasing the number of features given as input to the classifier over a given threshold, which depends on the number of training samples and the kind of classifier adopted. The effectiveness of the classification algorithms depends on their sensitivity to both the large spatial variability of the signatures of land-cover classes and the Hughes phenomenon.

Unsupervised Learning Classification. Unsupervised Learning classification does not require any class scheme information in advance, compared with supervised classification that scholars could select features and characteristics for the classes of interest. Unsupervised learning approach checks the digital information for pixels and breaks them into clusters or the most general natural spectral groupings. Cluster analysis

is the most common used unsupervised method, which could efficiently find the hidden pattern and group in data.

Canty and Nielsen (2006) proposed an unsupervised classification of change and no-change pixels with the fuzzy maximum likelihood estimation (FMLE) method, which allowed for hyper-ellipsoidal clusters and clusters of various sizes, and included a criterion for choosing the best number of classes. This method combined two processing capabilities that one capability manages the automatic detection issue of multiple changes while the other allows utility of spatial contextual information detected by a Markovian formulation.

Semi-Supervised Learning (SSL) Classification. Semi-Supervised classification methods utilize both training data and unlabeled samples in the learning phase in order to obtain a general decision function that can take into account both the information present in the training set and the structure of all data in the feature space (Bennett & Demiriz, 1998; Patra, Ghosh S., & Ghosh A., 2007).

Patra et al. (2007) used a context-sensitive semi-supervised change-detection technique based on multilayer perceptron (MLP) that automatically discriminates the changed and unchanged pixels of difference image. The initial network is trained by a small set of labeled data, and the unlabeled patterns are iteratively processed by the MLP to obtain a soft class label for each of them. The experimental results confirm the effectiveness of the SSL technique which outperforms the standard optimal-manual context-insensitive Manual Trial and Error Thresholding (MTET) method and K-means technique.

Jun and Ghosh (2011) propose a Gaussian process expectation maximization (GP-EM) algorithm, a spatially adaptive semi-supervised learning algorithm. In the GP-EM, spatially varying parameters of each Gaussian component are obtained by Gaussian regressions with soft memberships. Jun and Ghosh experimented on temporally separate training and test data (hyperspectral images by the NASA EO-1 satellite) in Botswana, South Africa, and showed superior results compared to other baseline algorithms.

Active Learning (AL) Classification. Active Leaning exploits the user-machine interaction, using an optimized training set and the user's effort to build the set to decrease the classifier error simultaneously. Active Leaning is an alternative to passive learning which is the standard approach adopted for the definition of a training set in RS, and based on the application of statistical sampling procedures that exploit the knowledge of the application domain for extracting ground reference samples without considering any interaction with the adopted supervised classifier (Tuia, Ratle, Pacifici, Kanevski, & Emery, 2009; Mitra, Shankar, & Pal, 2004).

Tuia et al. (2009) proposed an active learning classification framework for VHR QuickBird images and on AVIRIS Hyperspectral images. They utilize the Support Vector Machine (SVM) to develop an algorithm and a state-of-the-art active learning technique by controlling on the composition of the training set and choosing the most worth pixels. In Mitra et al.'s study (2004), the unlabeled sample that was closest to the classification boundary of each binary SVM in a One Against-All (OAA) multiclass architecture was considered as the most informative, and therefore included in the current training set at each iteration of the AL process. Jun, Vatsavali, and Ghosh (2009) used uncertainty sampling based active learning methods to classify the Advanced Wide Field Sensor

(AWiFS) data in Gaussian Process with a fewer number of samples. The active learners achieved better accuracies than passive learners in the experimental results.

National Agriculture Imagery Program (NAIP)

NAIP is a program to obtain high spatial solution aerial photographs during vegetation peak growing time period to maintain the common land unit boundaries and assist with farm programs. The NAIP imagery data consist of a total of 330 000 scenes covering the entire United States landscape.

Supported by USDA Farm Service Agency (FSA), NAIP has used film or digital cameras on aircraft to acquire signals. Both film and digital cameras require rigid calibration specification. From year 2003 to 2009, NAIP used both film and digital cameras, which have a nominal scale of 1:40,000. After 2009, most NAIP images have been acquired with digital sensors instead of film cameras. All individual tile aerial photographs and the resulting mosaic are rectified in the UTM coordinate system, NAD 83, and cast into a single predetermined UTM zone. Digital ortho quarter quad tiles (DOQQs) or as compressed county mosaics (CCM) are available as NAIP products.

The spatial resolution has been improved by new equipment updated, and differs by states in different years. The default of spectral resolution is four-bands, containing natural color (red, green, blue), and near-infrared bands. Radiometric resolution of NAIP imagery is 8-bit that shows the brightness values. In year 2002 to 2006, most states have 2-meter spatial resolution and four-band NAIP imagery. During this period, 1 meter spatial aerial photo is available for the year of 2005. From year 2007 to 2015, most states have 1-meter spatial resolution and four-band NAIP imagery, and few states, such as

New York State and Wyoming State, half-meter spatial resolution imagery could be acquired (NAIP Coverage 2002 - 2015).

NAIP imagery application mainly focuses on planning and environmental fields. Li and Shao (2014) introduced an object-based method that identified land use and land cover types from one-meter NAIP images and 5-foot digital elevation model. Li and Shao (2014) used principal component transformation to reduce the spectral dimension of NAIP aerial photographs. Then a hierarchical rule-based classifier was formed based on the image segmentation. Using additional ancillary data could help generate more accurate land use classification.

Using NAIP imagery, Qiu, Wu, and Miao (2014) applied expert knowledge based classification method combined with incorporated road and parcel GIS data to generate and urban feature map of Nixa city, Missouri. Dinger, Zourarakis, and Currens (2007) utilized NAIP imagery in 2014 summer to locate cover-collapse sinkholes.

Davies et al. (2010) extracted western juniper cover from NAIP imagery and explored the relationships between juniper cover at stand closure and environmental indices. Kirk concluded that NAIP imagery can be a valuable tool to estimate juniper cover over large areas effectively which makes landscape-scale restoration more feasible.

Ortho photography from NAIP is a valuable data source for land use and land cover classification in the United States of America. This agriculture oriented imagery program covers nationwide and avoids the negative effect of clouds. The one-meter spatial resolution imagery is free for public to obtain online with three visible color bands, and low cost for the Near Infrared spectral band. The update frequency is one year every summer period. However, there are challenges for using NAIP imagery e.g.

Shadow impact, registration error, radiometric normalization, and calibration (Maxwell, Strager, Warner, Zégre, & Yuill, 2014).

STUDY AREA AND DATA PROCESSING

Study Area

Table Rock Lake (TRL) is an artificial lake located at southwestern Missouri and northwestern Arkansas. TRL is formed by construction of Table Rock Dam which built by the U.S. Army Corps of Engineers on the White River between year 1954 to 1958. Table rock lake region (TRLR) becomes one of the popular travelling destination attracting visitors nearby and around nation. The land use and land cover is an important factor for local government, city planners and commercial analysts to make polices and development decisions. This review includes a brief history over TRL region before and after Table Rock Dam construction over last century, land use phenomenon, population growth and local business development recent years.

At the beginning of 20th century, White river flow through TRLR with few residential area and human settlement. The only human activities here are little seasonal agriculture, hunting and fishing business. From the 1920s to the 1950s, a novel called The Shepherd of the Hills by Harold Bell Wright described Ozarks attracted visitors to fish in TRLR, and then retailers started to settle down in TRLR to provide basic daily supplies and foods. After Table rock dam constructed to protect local citizens and land from annual water flooding, TRLR became more stable and safer for living. Downstream from dam is still flowed by white river, now called as Table Rock River. The cold water with more nutrient soil and microbes raised up is discharged from Table Rock Dam and bred various types and a huge amount of fishes. Therefore travelling and fishing business raised up in this region. Branson city, Missouri is a typical city formed during the 1950s.

In 1992, Trees and forest comprise the greatest percentage of land use and land cover types in the watershed, followed by pasture land, range land, noncultivated cropland, urban, water, roads, miscellaneous and cultivated cropland. In 1997, deciduous forest still comprises the greatest percentage of land use and land cover types in this watershed, followed by mixed forest, grassland, water, cropland and urban.

This study focuses on three rectangular areas in the Stone and Taney County of Missouri along the Table Rock Lake. They are named after the main town occupied in each site, including Table Rock Village, Indian point and Kimberling City. The three study areas are located between 36°39'54.5" and 36°32'16.0" N latitude and 93°25'57.9" and 93°15'57.7" W longitude. All three sub study areas (Figure 1) are typical lakeside regions which are constituted with natural landscape and artificial construction.

Table Rock Village area is manually chosen as an extension of southwestern Branson City and Hollister city. As of the 2010 census, there are 229 people, 96 households, and 69 families residing in the village. The population density was 1,094.1 people per square mile (421.0/km²).

Kimberling City area combines Kimberling city in north and couples of residential neighborhood cross the table rock lake in the south. There were 2,400 people, 1,147 households, and 774 families residing. The population density was 701.8 inhabitants per square mile (271.0/km2) (census 2010).

Indian Point area includes most area of Indian point, and surrounding lake area and forest. There were 528 people, 243 households, and 159 families residing in the village. The population density was 187.9 inhabitants per square mile (72.5/ km2) (census 2010).

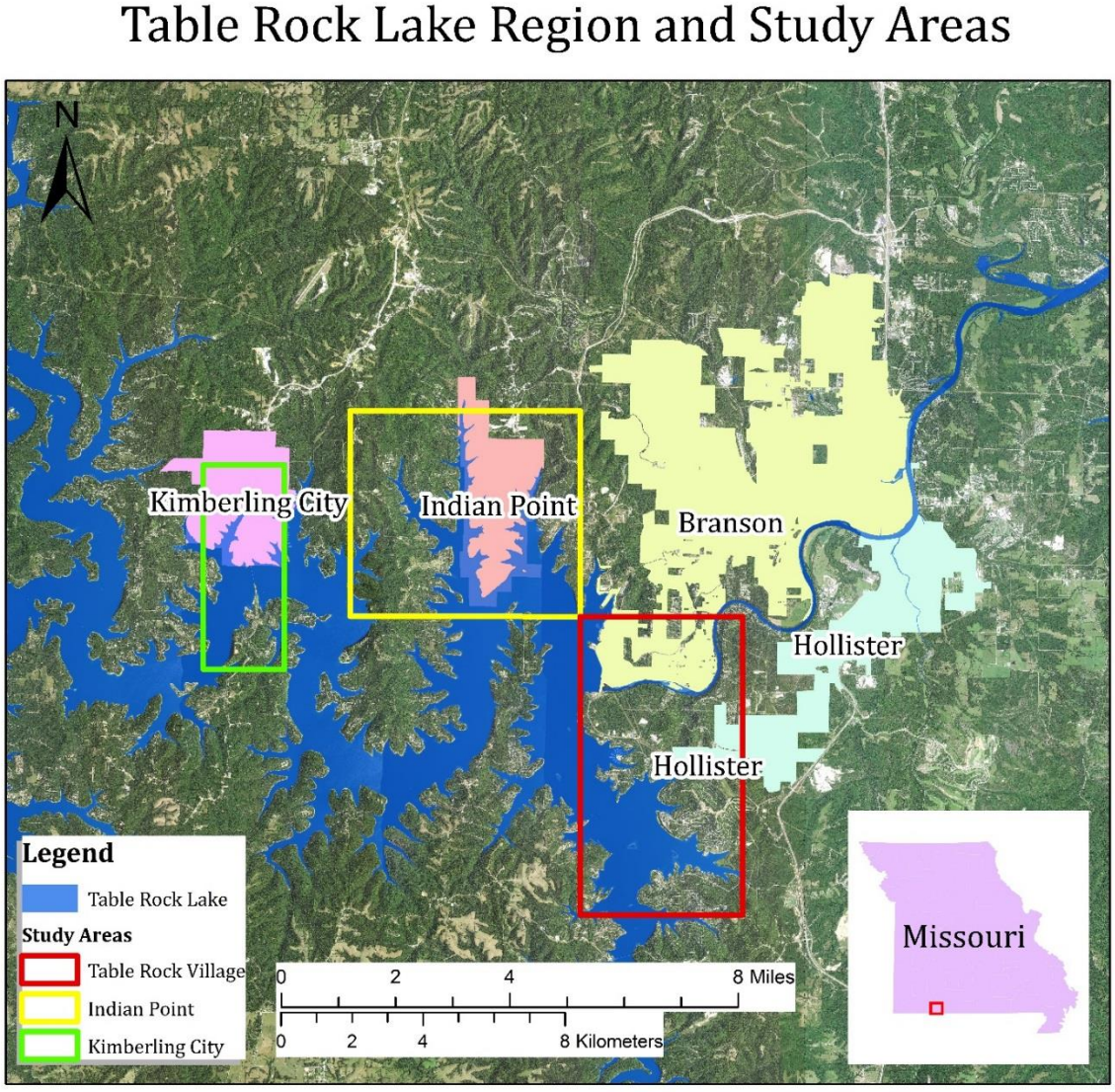

Figure 1. Study area of Table Rock Lake Region

NAIP Imagery

Digital Orthophoto Quarter Quads (DOQQs) of the study area were obtained from Missouri Spatial Data Information Service (MSDIS) in GRID Stack 7.x format. The data has already been rectified to UTM 15N projection (GRS1980) and geographic coordinate reference is GCS North American Datum 1983. Four adjacent individual resampled mosaics (Figure 2) of Stone and Taney County covering all sub study areas. The images were taken on July 18, 2009, July 26, 2010, August 21, 2012 and July 12, 2014. Each DOQQs is one meter spatial resolution and includes four spectral bands (RGB visible bands and near infrared band) in 8 bits or 16 bits.

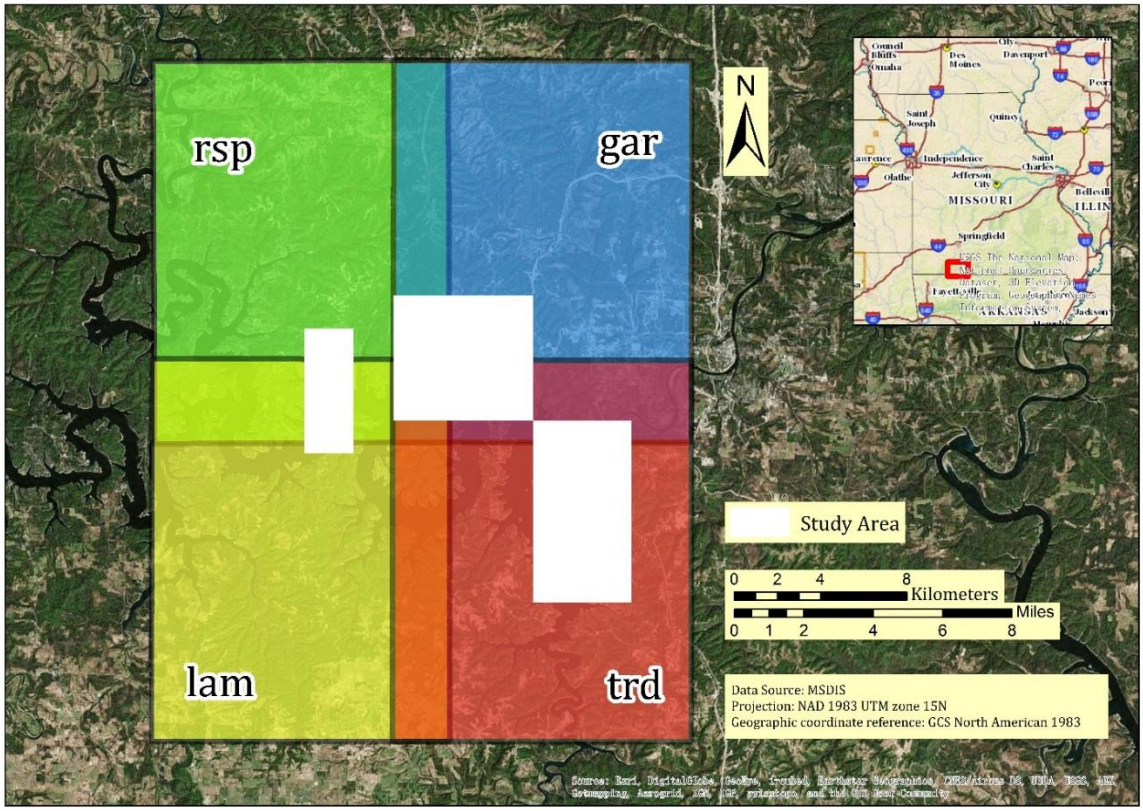

Figure 2. Primary NAIP imagery from MSDIS

The images were preprocessed in *ArcGIS 10.2* and *ENVI Classic (32-bit)*. First all original GRID Stack 7.x files were transformed into GeoTIFF file. Resampled mosaics in the same year were merged into an overview image first and then resized to the target study areas by the polygon shapefile of Table Rock Village, Kimberling City and Indian Point. Image enhancement techniques were utilized for better and easier artificial recognition of land features during collecting training and test samples. Linear contrast stretch for each image was applied, which required trial and error process to adjust a relative obvious visualization in spectral histogram plot. Table 1 is a list showing the processed aerial imagery for classification and change detection.

Table 1. Preprocessed NAIP aerial imagery for classification.

#	Study Area	Year	Date	Total bands	Pixel Depth (bit)
1	Table Rock Village	2009	18 July	4	8
2	Table Rock Village	2010	26 July	4	8
3*	Table Rock Village	2012	21 August	4	16
4	Table Rock Village	2014	12 July	4	16
5	Kimberling City	2009	18 July	4	8
6	Kimberling City	2010	26 July	4	8
7	Kimberling City	2012	21 August	4	16
8	Kimberling City	2014	12 July	4	16
9	Indian Point	2009	18 July	4	8
10	Indian Point	2010	26 July	4	8
11	Indian Point	2012	21 August	4	16
12	Indian Point	2014	12 July	4	16

Note: * This image was selected for the first stage of finding the optimal classification workflow. Other data were utilized in the second stage.

METHODOLOGY

This study includes two stages. In the first stage the image of 2012Table Rock Village was used as an experiment target to compare six classification approaches in terms of the accuracy and efficiency. During the second stage, the optimal methods identified in the first stages was applied to classify the rest 11 aerial photographs and detect the LULCC for three sub study areas. Figure 3 shows the object-based classification workflow (Miao, 2015). At each classification image we selected training samples artificially by visualized interpretation in a 2-level class scheme. A two-step segmentation algorithm was applied on the aerial photos. Nineteen object features were selected and calculated for all training objects, and then were input into each classifier. Accuracy assessment was conducted to compare classification methods, and the post-classification comparison is applied to detect LULC changes.

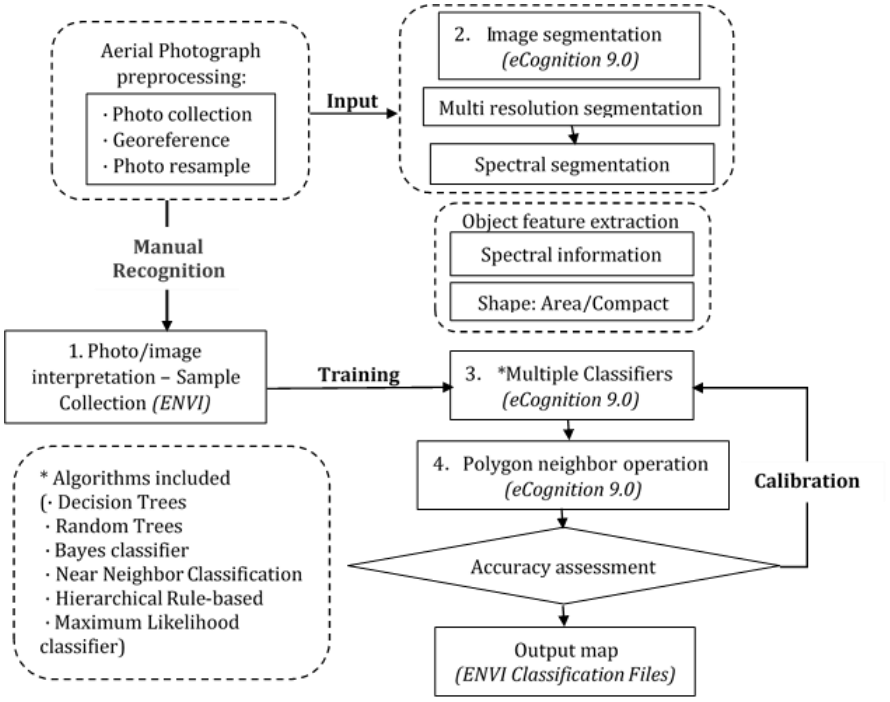

Figure 3. Object-based Image Classification Workflow

Training and Test Samples Collection

All samples were collected through visual interpretation using *ENVI Region of Interest (ROI)* tool on a per-pixel base to reduce redundancy and spatial-autocorrelation. Classification scheme was defined from sample collection into 8 LULC types including water, trees/forest, grass/lawn, bare ground land, buildings, paved road, parking lots and shadows, which were then reclassified into other land types. Table 2 shows the classification scheme and the detailed interpretation characteristics. False color visualization and expert's experiences were used in this step.

The classification result can be influenced by the size of representative training samples, which requires a systematic, random and stratified random sampling strategy. Lack of training samples could lead to greater classification accuracy discrepancies than what classification algorithms introduce. However, artificial sample collection is both time-consuming and labor-intensive. There is an acknowledged standard that the training sample size for each class should not be fewer than 10–30 times the number of bands (Van, McVicar, & Datt, 2005). In real practice, there are only four spectral bands, so 50 to 150 plots were selected for each land cover, while some land types such as parking lot sites could not count to 50 due to their original limited number.

For the first stage of using Table Rock Village 2012 dataset, both training and test samples for seven land types (shadows are not counted) were collected in the form of polygons and converted to shapefile. A total of 219118 pixels training samples and 136371 pixels validation samples were extracted from 640 different sample sited used in this study as showed in (Table 3) for Table Rock Village year 2012. For the second stage, only training samples were collected (Table 4, Table 5 and Table 6). Finally, all training

sample sites were assigned to input into classification segments and all validation sample pixels were used to make the accuracy assessment.

Table 2. Classification scheme for detection of LULC type from aerial photographs

#	Class name		Class Description
1	Water		Table Rock Lake, White River, reservoirs and residential swimming pools, ponds. Objects are darker than other land types.
2	Vegetation	Trees/Forest	Large area and high density of tree-crown forest occupied, including different kinds of arbors, bushes and mixed category. Individual trees planted separately in residential areas.
		Grass/Lawn	Land of short, mown grass in yard, garden or wild mixed vegetation areas.
3	Bare Ground		Land mainly covered by sand, soil and rocks that has limitation ability to support vegetation and life. Bare ground might be caused by construction preparation or forest desolation.
4	Impervious	Buildings/Roof	Residential houses, commercial constructions and piers. Rectangular polygons with high density in the urban core and low density with bare ground or lawn in urban expansion. The color of roofs can be white, grey, brown, red and mixed color in study areas.
		Paved Road	Transition area covered with concrete, stones, bricks and shows consistent linear feature.
		Parking Lot	Transition area covered with pitch and concrete, which is adjacent to residential buildings and vehicles could be identified in this field.
5	Shadow		Darker objects on the bare ground, lawn, forest, parking lots and paved roads caused by related higher elevation of artificial structures and trees.

Table 3. The number of sites and sample pixels for Table Rock Village 2012

Class Name	Training		Test	
	Sites(polygons)	Subtotal	Sites(polygons)	Subtotal
Water	100	55657	109	41109
Trees/Forest	101	8543	109	7946
Grass/Lawn	51	7917	106	8510
Bare Ground	73	41970	98	6292
Buildings/Roof	100	54192	120	28772
Paved Road	58	31272	54	23160
Parking Lot	38	19567	44	20582
Total	521	219118	640	136371

Table 4. The number of sites and sample pixels for Table Rock Village (2009-2014)

Class Name	2009		2010		2012		2014	
	Sites	Subtotal	Sites	Subtotal	Sites	Subtotal	Sites	Subtotal
Water	57	118387	101	58566	100	55657	86	9235
Trees/Forest	109	18704	109	20909	101	8543	104	8089
Grass/Lawn	92	13937	102	14291	51	7917	100	2830
Bare Ground	65	10456	63	5375	73	41970	41	6193
Buildings/Roof	102	35611	113	24400	100	54192	135	57115
Paved Road	44	17457	55	27233	58	31272	47	17522
Parking Lot	23	11965	35	13784	38	19567	18	17522
Shadow	68	1620	NA	NA	NA	NA	103	3733
Total	560	228137	578	164558	521	219118	634	122239

Table 5. The number of sites and sample pixels for Kimberling City (2009-2014)

Class Name	2009		2010		2012		2014	
	Sites	Subtotal	Sites	Subtotal	Sites	Subtotal	Sites	Subtotal
Water	52	19456	106	25729	24	10981	64	30515
Trees/Forest	84	13009	101	9617	72	6778	100	48141
Grass/Lawn	59	5904	100	6287	20	1101	72	9044
Bare Ground	49	6265	56	4492	36	2902	48	2760
Buildings/Roof	109	40490	83	37811	61	21756	127	5808
Paved Road	37	11152	33	14626	10	4519	46	2909
Parking Lot	26	18676	14	13702	18	18075	21	6132
Shadow	58	832	NA	NA	NA	NA	103	3321
Total	474	115784	493	112264	241	66112	581	108630

Table 6. The number of sites and sample pixels for Indian Point (2009-2014)

Class Name	2009		2010		2012		2014	
	Sites	Subtotal	Sites	Subtotal	Sites	Subtotal	Sites	Subtotal
Water	79	90812	93	37764	96	35812	30	14704
Trees/Forest	108	14316	110	19201	106	7640	102	24846
Grass/Lawn	68	9932	104	11602	63	3626	29	2411
Bare Ground	62	7194	46	5169	103	6058	51	2802
Buildings/Roof	113	32783	130	31689	67	18923	71	19897
Paved Road	51	16809	33	9983	60	14628	37	14428
Parking Lot	12	8049	15	8354	21	10827	15	25357
Shadow	NA	NA	NA	NA	NA	NA	109	8094
Total	493	179895	531	123762	516	97514	444	112539

Image Segmentation

Multiresolution segmentation and spectral difference segmentation in eCognition Developer software were employed to segment the image pixels into a set of discrete non-overlapping regions on the bases of internal homogeneity criteria. Different types of land cover, particularly impervious area and vegetation areas in various sizes and shapes

in the image, could be extracted by a combination of two segmentation steps. For the segmentation process, three visible and near infrared bands were considered.

Multiresolution image segmentation is a region-growing algorithm from bottom to top which, starting from each image pixels, merges the most resembling adjacent regions until the internal heterogeneity of the final object does not exceed the default set threshold factors (Benz et al., 2004). Trial and error technique was attempted to evaluate the influence caused by different segmentation parameters. Tests for nine different scales (10, 20, 30, 40, 50, 60, 70, 80 and 90) were performed to locally minimized heterogeneity between neighboring objects. Shape weighted parameter was modified under 20 scale parameter. The optimal scale, shape and compactness parameters may differ depending on the type of landscape and spatial resolution of input data. The following parameters (Table 7) were last used for the segmentation of Table Rock Village in 2012, and the study area was subdivided into 903,815 objects of consistent shape.

Based on the image layer intensity mean values, spectral difference segmentation algorithm is used to merge spectrally similar image objects produced by previous over-segmented step. Large homogeneous areas, such as water body and vegetation, can be created regarding spectral difference. The maximum spectral difference parameter was set at 10, then the segmentation result was merged to 581,945 objects.

Table 7. Segmentation parameters for Table Rock Village 2012

Step 1 - Multi-resolution segmentation	Scale	Color	Shape	Compactness	Number of Objects
	10	0.8	0.2	0.5	903,815
Step 2 - Spectral difference segmentation	Maximum spectral difference				Number of Objects
	10				581,945

Image Classification

Image classification is the core procedure in this study. Six algorithms were used to classify composite imagery of Table Rock Village in year 2012, including a pixel-based maximum likelihood classification, and five object-based classification methods which are random tree classifier, decision tree classifier, nearest-neighbor classifier, Bayes classifier and a hierarchical rule-based set approach. Table 8 is served as a general review guide listing and comparing these six algorithms.

The pixel-based maximum likelihood is conducted in *ENVI IDL* which only considers four spectral features under pixel level and used as a reference compared with object-based classifier here. Training samples in pixels with four spectral bands were utilized as input value to make maximum likelihood classification.

In the object-based level, the outputs from the image segmentation are individual polygons (objects). Training samples were thematically assigned into segment result in *eCognition,* and features for all of the training segments were extracted and used as input for the object-based classifiers. The features were divided into three categories, (a) customized spectral features that are common utilized to classify vegetation (Normalized Difference Vegetation Index), water (Normalized Difference Water Index), bare ground land (Soil Brightness Index) and buildings (Burn Area Index), (b) four means and standard deviations and brightness value respectively calculated from the band *i* values of all n pixels forming an image object (polygon), (c) six related shape features. In total, nineteen spectral and shape attributes of each object are selected by their possible influences for land type recognition, as defined in Table 9. Random tree, decision tree,

nearest-neighbor classifier and Bayes classifier utilized the same features and training segments for classification.

Table 8. A general description of different classification methods

	Methods	Description and property
Pixel-based	Maximum likelihood	It allocates a case to the class with the highest probability of membership. Widely applied in low spatial resolution imagery. Maximum likelihood classifier only considers four spectral features under pixel level and is used as a reference compared with object-based classifier in this study.
Object-based	CART (Decision tree)	This algorithm examines all possible splits of the data and selects a split threshold value of the explanatory variable that produces maximum dissimilarity, or deviance, between the resulting subsets.
	Random tree	A Random trees classifier uses a number of decision trees to improve the classification rate. It can be easily migrated to a parallel computing environment.
	Nearest-neighbor	This classifier is a non-parameter machine learning algorithm: given a feature vector, the system finds the nearest neighbors among the training vectors, and uses the categories of the neighbors to determine the category of this test vector (object). Euclidean distance is used.
	Bayes classifier	Based on Bayes theorem, this Classifier calculates the posterior probability and assumes class conditional independence. Uncomplicated iterative parameter estimation makes it particular useful for very large datasets.
	Hierarchical rule-based approach	Hierarchical rule-based approach is semi-automated and created by expert knowledge combining membership function classifier (NDVI threshold) and machine learning algorithms. Small number of labeled training data is available. It requires manual work in the process.

To classify image objects using above four classifier in eCognition 9.0, we need to define the feature space, define training samples (objects), classify, review the outputs,

and optimize the classification. The classification procedure uses a set of samples that represent different classes in order to assign class values to segmented objects. The procedure therefore consists of two steps: first to teach the system by giving it certain image objects as samples, and second to apply the trained scene in their feature spaces to classify the ensemble segments.

Hierarchical rule-based approach is a semi-automated approach created by expert experience that combines membership function classifier and machine learning algorithms. The approach consists of two steps in a fuzzy decision tree. First, user's expert knowledge and understanding about customized spectral features are used to define basic rules to classify level 1 classes of water body, vegetation, shadows and impervious surface land. In this step, NDVI and brightness value were selected as membership threshold factor to assign classification. For example, if NDVI < -0.2, the water body mask would be created, and vegetation mask created if NDVI > 0. The membership function defines the ranges of feature values that decide whether the objects belong to a particular land type or not. The membership function only depend on a single or a combination of parametric rule, which could follow a normal distribution or a specific threshold value. The second step is to classify level 1 scheme into level 2 classes. For vegetation, nearest-neighbor classifier with feature space of mean and standard deviation for green and blue band is utilized to separate trees/forest and grassland. For impervious surface, random tree classifier with selected features (BAI, brightness, area, length/width, density and rectangular fit) are used to reclassify impervious surface into building, parking lot, bare ground and paved road.

Table 9. Definitions of nineteen spectral, shape attributes extracted from each object

Feature	Name	Number	Description
Customized spectral features	Normalized Difference Vegetation Index (NDVI)	1	$\text{NDVI} = \frac{(NIR - R)}{(NIR + R)}$
	Normalized Difference Water Index (NDWI)	1	$NDWI = \frac{(G - NIR)}{(G + NIR)}$
	Soil Brightness Index (SBI)	1	$\sqrt[2]{R^2 + NIR^2}$
	Burn Area Index (BAI)	1	$BAI = \frac{(B - NIR)}{(B + NIR)}$
Spectral	Brightness	1	$Brightness = \frac{R + G + B + NIR}{4}$
	Average Band Value	4	$B_i = \sum BV/n$, where n is the number of pixels and B is the value for each pixel of layer i.
	Standard deviation Band Value	4	$\sigma_L = \sqrt{\frac{1}{n-1} \cdot \sum_{i=1}^{n} (C_{Li} - \bar{C}_L)^2}$
Spatial	Area	1	True area covered by one pixel times the number of pixels forming the image object.
	Length/Width	1	Length of bounding box divided by width of bounding box.
	Compactness	1	$C = 4\pi \cdot A/P^2$, where P is the perimeter.
	Density	1	The area covered by the image object divided by its radius.
	Rectangular Fit	1	Ratio of the area inside the fitting equiareal rectangle divided by the area of the object outside the rectangle.
	Roundness	1	$Roundness = 4\pi \cdot \frac{Area}{convex\ perimeter^2}$

Neighbor Objects Operation

Neighbor objects operation includes assigned reclassification for shadows and merge operation. After extracting shadow areas, they should be assigned to the corresponding land cover class. Visual inspection of the image reveals that shadows cast by buildings belong to either lawns or parking lots. A few buildings have multi-level roofs and the shadow of the higher roof covers part of the lower roofs. Other shadows might be generated from tall trees. The trees' shadow could project on near trees in the high density forests or event on the surrounding lawn by individual tree crowns. Rule-set is developed to assign shadows into land type of forest, lawn, buildings, parking lots and bare ground. The feature *existence of neighbor objects* and *adjacent radio (defined as adjacent border divided by object' border)* is utilized to define the assign classification threshold value. If the shadow is adjacent to building/roof object(s), it could be assigned to parking lots, lawns or buildings (building adjacent radio comes to 1). If the shadow is adjacent to trees object(s), it could be assigned to bare ground, lawns or tree/forest (adjacent radio comes to 1). It should be noted this step is fuzzy and generated by expert's experience. Shadows could also belong to road as well. However, in this study, only images in the year 2014 and 2009 have small areas covered by shadows which do not have a significant effect on the classification accuracy of the entire photo.

The neighboring same-class polygons are merged to reduce the number for over segmented polygon which should belong to a consistent object, such as roofs and complete water body.

Pixel-based Accuracy Assessment

Pixel-based accuracy assessment was used to compare the classification results for six methods above at every pixel in Table Rock Village 2012 images with a reference source and a ground truth test samples collected at first. Banko (1998) suggested that a minimum number for 75 or 100 sample points for each LULC category in the confusion matrix be collected for the accuracy assessment of large-area image classification. As Table 3 shows, 640 plot samples were collected in 136, 371 pixels that led to approximately 19, 480 data points per class (7 total classes) for the accuracy assessment. The results of accuracy assessment can be analyzed and evaluated by overall classification accuracy and Kappa coefficient. Error matrices were produced to show the contingency of the class to which each pixel truly belongs (columns) on the map unit to which it is allocated by the selected analysis (rows). Raster format of classification results was extracted from *eCognition 9.0* and confusion matrix by regions of interest (ROI) in *ENVI-classic* was utilized to generate accuracy assessment.

Post-classification Change Detection

Overall classification results statistics and pixel-based "from-to" change confusion matrix were employed to detect the change in the study area. Overall classification statistics aims to identify how main land cover type changed quantitatively between year 2009 to 2014. Bare ground, buildings, parking lots and roads were merged into a new higher level class called impervious surface. The combined impervious surface was recognized as a key indicator to assess urban environment. Then the areas of four main natural and artificial land types, including water, trees, grass and impervious

surface, were calculated in meters and percentage of overall images. More specifically, post-classification confusion matrix was executed to compare initial year 2009 and ending year 2014. Both of the change detection techniques were run in *ENVI Classic*.

RESULTS AND DISCUSSION

Classification of multi-temporal images for three sub study fields are extracted by object-based image analysis approach (Figures in Appendix A). In this chapter, three sections aim to provide the results for the three research objectives. Different algorithms were utilized to classify land use and land cover of the Table rock village in year 2012, and compared by accuracy and efficiency. Overall land types statistics results are in the second section. The third section shows the change detection results by year 2009 and 2014.

Comparison of Supervised Classification Results

During the classification process, semi-automated hierarchical rule-based decision tree requires a long time (two hours) to use expert knowledges of setting the membership function threshold values for each class type. For other automated supervised classification, both object-based and pixel-based methods do not require human participation in the process. Random tree, decision tree, Bayes classifier and maximum likelihood saved time less than ten minutes, while nearest-neighbor classifier took 90 minutes to run.

A comparison of six algorithms for Table Rock Village year 2012 image in Table 10 includes the general accuracy of pixel-based overall accuracy in percentage, Kappa Coefficient, and accuracy for seven classification types (Tables in Appendix B). Compared with overall accuracy and Kappa Coefficient, random trees classifier comes to the first, and followed by Hierarchical rule-based classifier, Nearest-neighbor classifier,

decision tree at the mid-level, and then Bayes classifier algorithm and pixel-based maximum likelihood classification approach. The correlation between overall accuracy in percent and Kappa Coefficient indicates the Random Tree is the most accurate algorithm to classify land use and land cover type of one meter four bands NAIP aerial imagery with same selected object features in this area.

Classification accuracy for specific classes is also compared. For water body, semi-automatic hierarchical rule-based classifier achieves 99.82%, and followed by Nearest-neighbor classifier (98.65%), Bayes classifier (92.52%), decision tree (91.61%), random tree (90.71%) and pixel-based maximum likelihood classification (78.66%) at last.

In vegetation classification, for trees and forest, semi-automatic hierarchical rule-based classifier achieves the highest 95.68%, and followed by pixel-based maximum likelihood classification (92.95), random tree (93.68%), decision tree (89.16%), Nearest-neighbor classifier (88.71%), and Bayes classifier (81.80%) at last. For grass and lawn, random tree achieves 98.65% at first, and followed by decision tree (98.07%), pixel-based maximum likelihood classification (95.12%), semi-automatic hierarchical rule-based classifier (85.25%), Bayes classifier (81.80%), and Nearest-neighbor classifier (76.64%) at last. The results of trees and grass did not show homogeneity, but random tree classifier still is the best for grass and second best for trees which indicate the best classification method for vegetation extraction.

Table 8. Comparison of six algorithms in terms of accuracy

Algorithm	General Accuracy		Detail Accuracy for Each Class (%)						
	Overall Accuracy (%)	Kappa Coefficient	Water	Trees/ Forest	Grass/ Lawn	Bare Ground	Building/ Roof	Paved Road	Parking Lot
Random Trees	87.696	0.8479	90.71	93.69	98.65	83.11	78.3	95.3	80.8
Decision Trees	82.777	0.7864	91.61	89.16	98.07	68.8	70.84	83.7	76.24
Nearest-neighbor	83.063	0.7911	98.65	88.71	76.64	74.7	67.97	86.35	72.33
Bayes classifier	73.771	0.6791	92.52	90.91	81.8	87.6	29.81	78.8	77.84
Hierarchical rule-based classifier	83.826	0.8001	99.82	95.68	85.25	88.76	70.21	91.51	55.56
Maximum likelihood (pixel based)	70.916	0.6453	78.66	92.95	95.12	72.22	31.67	88.98	70.97

In bare ground, semi-automatic hierarchical rule-based classifier achieves the highest 88.76%, and followed by Bayes classifier (87.60%), random tree (83.11%), Nearest-neighbor classifier (74.70%), pixel-based maximum likelihood classification (72.22%) and decision tree (68.80%) at last. In impervious surface land classification, for buildings and roofs, random tree achieves the highest 78.30%, and followed by decision tree (70.84%), semi-automatic hierarchical rule-based classifier (70.21%), Nearest-neighbor classifier (67.97%), pixel-based maximum likelihood classification (31.67%) and Bayes classifier (29.81%) at last. For paved roads, random tree achieves the highest accuracy 95.30%, and followed by semi-automatic hierarchical rule-based classifier (91.51%), pixel-based maximum likelihood classification (88.98%), Nearest-neighbor classifier (86.35%), decision tree (83.70%) and Bayes classifier (78.80%) at last. For buildings and roofs, random tree achieves 80.80%, and followed by Bayes classifier (77.84%), decision tree (76.24%), Nearest-neighbor classifier (72.33%), pixel-based maximum likelihood classification (70.97%) and semi-automatic hierarchical rule-based classifier (55.56%) at last. Although object-based classification methods do not show with very high accuracy in impervious surface extraction, random tree classifier is relatively better than others.

Detailed classification accuracy for a single class type differs greatly so that most of algorithms classifying land cover type of water, vegetation and paved roads are larger than 85%. For buildings, bare ground and parking lots, their mean accuracy is smaller than 85%. In particularly, the highest accuracy of buildings is only 78.30%. Table 11 illustrates a detailed confusion matrix for the misclassification of different classes in the study site. Buildings are mainly misclassified by parking lots and bare ground. Bare

ground is mainly misclassified by parking lots and lawns. Parking lots are mainly misclassified by paved road and buildings. This phenomenon shows a weakness for object-based classification methods to extract artificial land types. This weakness could be caused by:

1) The genetic and intrinsic characteristic of bare ground and impervious surface is hard to distinguish. Some land cover types might include detailed sub types, for example building roofs could be classified into the roof with white, grey, brown and red color, while parking lots could be divided into pitch or dust surface. The samples collected for sub class types do not have representative spectral and shape features. So only relying on spectral information of the image hardly verify the difference between these classes. For the shape and texture features, concrete parking lots could be misclassified by concrete roads or buildings, because some target segments or polygons (objects) are very similar even by visual interpretation on the aerial photograph.

2) The parameters select' for segmentation is based on a single image in eCognition software. Although every experiment parameter has been manually adjusted by expert in each step and the result seems relatively optimal, the parameters still have limitations. The packaged software eCognition is a black box that users could only choose the given parameters in different steps like segmentation scale and classifier factors. It is hard to tell the exact algorithm behind and how it works.

3) Feature selection of training and targeting objects. Texture and context features are not involved in this experiment. Only 0.09% objects sample was trained to classify all polygons in the study site (521 of 581,945).

Table 9. Accuracy Assessment of Random Tree for Detailed Classes Results (Table Rock Village 2012)

Class	Lawn/ Grass	Water	Building/ Roof	Trees/ Forest	Bare Ground	Parking Lots	Paved Road	Total
Unclassified	0	0	0	0	0	0	0	0
Lawn/Grass	98.65	0	0.37	3.28	6.61	0	0.03	6.74
Water	0	90.71	0	0	0	4.3	0	28
Building/Roof	0	4.62	78.3	0.04	1.94	7.11	2.41	19.47
Trees/Forest	0.54	0	0.02	93.69	0	0	0.02	5.5
Bare Ground	0.73	0	6.84	0.86	83.11	0.36	0.85	5.57
Parking Lots	0.02	4.67	13.24	0	0.46	80.8	1.39	16.66
Paved Road	0.06	0	1.24	2.13	7.88	7.41	95.3	18.06
Total	100	100	100	100	100	100	100	100

To improve the classification accuracy, 1) Adding ancillary data to spectral bands of high resolution imagery over urban areas is critical for classifying spectrally similar classes such as buildings and traffic areas. Elevation information like Lidar data and digital elevation model (DEM) could help to separate higher objects (buildings) from other impervious surface land. Road network data could be available from the planning department. Combining with context and neighboring distance features could also improve the classification of buildings and bare ground. Specifically in Missouri, footprint dataset collected in year 2014 with high accuracy by MSDIS program of hundreds volunteers could assist to make a standard for classification of local buildings and roofs land types. 2) Open coded algorithms and dataset could be utilized in classification processes, which could show precise details of the algorithms, and be manually adjusted and controlled to find the optimal work process. 3) More training data could be collected in each imagery.

In summary, object-based image classification is commonly better than pixel-based method in accuracy assessment, and random tree classifier is a reliable and efficient method in this study. Random tree classification for spectral heterogeneity such as water, vegetation and impervious surface is better than deeper classification of impervious surface. However, ancillary data, open-code algorithms, and professional sample collection based on features can be considered to improve the classification workflow of NAIP imagery.

Overall Land Use and Land Cover Statistics Results

The figures in Appendix C show developed land use and land cover classification in Table Rock Village, Kimberling City and Indian Point area. Table 12, Table 13 and Table 14 show the LULC area statistical results in meter^2 and percentage for each study areas. Figure 4, Figure 5 and Figure 6 show the overall LULC change tendency based on multi-temporal imagery classification.

Table 10. LULC supervised classification details (m^2 and percentage) in Table Rock Village

	2009	2010	2012	2014
Water	11592889 (30.138%)	11609180 (30.181%)	11169041 (29.036%)	11373654 (29.565%)
Trees/Forest	16043130 (41.708%)	16172797 (42.045%)	15017353 (39.041%)	18436220 (47.924%)
Lawn/Grass	4591098 (11.936%)	4848069 (12.604%)	2774597 (7.213%)	2897497 (7.532%)
Bare Ground	1999394 (5.198%)	2075091 (5.395%)	4643712 (12.072%)	2250261 (5.849%)
Building/Roof	615997 (1.601%)	393967 (1.024%)	961534 (2.5%)	1377842 (3.582%)
Paved Road	2183490 (5.676%)	2079315 (5.406%)	2889304 (7.511%)	1451496 (3.773%)
Parking Lot	1435780 (3.733%)	1278247 (3.323%)	1010142 (2.626%)	661015 (1.718%)
Impervious surface	4235267 (11.010%)	3751529 (9.753%)	3899446 (12.637%)	3490353 (9.073%)

For Table Rock Village in 2009 to 2014, trees and forests comprises the greatest percentage (more than 40%) of land use and land cover types in the study site, and followed by water body (around 30%), impervious surface and grass and lawns. Specifically paved roads occupied the greatest parts of in impervious classes, then followed by parking lots and buildings.

Trees and forest cover has become more extensive. Although the trees cover looks like a slight decrease between year 2010 to 2012 (42.045% to 39.041%), the increase between year 2012 to 2014 from 39.041% to 47.924% is obvious and clear. Water cover kept relatively stable during this period. Grass and lawns and impervious surface experienced a slight decline from 2009 to 2014. It indicates that parts of artificial land and grass land has been covered to trees and forest.

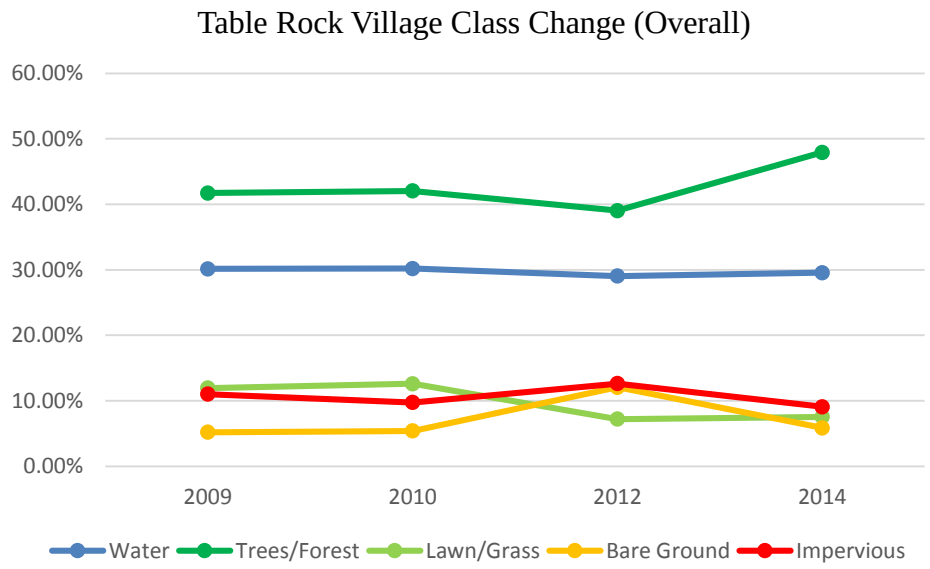

Figure 4. LULC change tendency of Table Rock Village (2009-2014)

For Kimberling City from 2009 to 2014, water body comprises the greatest percentage of land use and land cover types in the study site, and followed by trees and forest, grass and lawns and impervious surface. Specifically paved roads occupied the greatest parts of impervious classes, then followed by buildings and parking lots.

All land use classes seem not change at all from initial year 2009 to final year 2014. However, trees, grass and impervious surface fluctuated. Figure 5 shows

impervious surface decreased in first and third time gaps. A great increasing for impervious showed up between the year 2010 to 2012, which was contributed by bare ground extension. On the contrary, forests and lawns increased first and decreased a lot during year the 2010 to 2012. We could assume this change phenomena caused by natural and environmental conditions.

Table 11. LULC supervised classification details (m^2 and percentage) in Kimberling City

	2009	2010	2012	2014
Water	4883569 (36.985%)	4826932 (36.556%)	4870378 (36.885%)	4730845 (35.828%)
Trees/Forest	4320439 (32.72%)	4655068 (35.255%)	4185219 (31.696%)	4294258 (32.522%)
Lawn/Grass	1490319 (11.287%)	1573419 (11.916%)	771039 (5.839%)	1612794 (12.214%)
Bare Ground	747765 (5.663%)	822546 (6.229%)	1710614 (12.955%)	925067 (7.006%)
Building/Roof	346961 (2.628%)	484804 (3.672%)	443583 (3.359%)	677900 (5.134%)
Paved Road	1030567 (7.805%)	664885 (5.035%)	755588 (5.722%)	278760 (2.111%)
Parking Lot	384520 (2.912%)	176486 (1.337%)	467719 (3.542%)	684516 (5.184%)
Impervious	1762048 (13.345%)	1326175 (10.044%)	1666890 (12.623%)	1641176 (12.429%)

For Indian Point from 2009 to 2014, trees and forests comprises more than half percentage of land use and land cover types in the study site, and followed by water body (25%), grass and lawns and impervious surface. Specifically paved roads occupied the greatest parts of in impervious classes, then followed by buildings and parking lots.

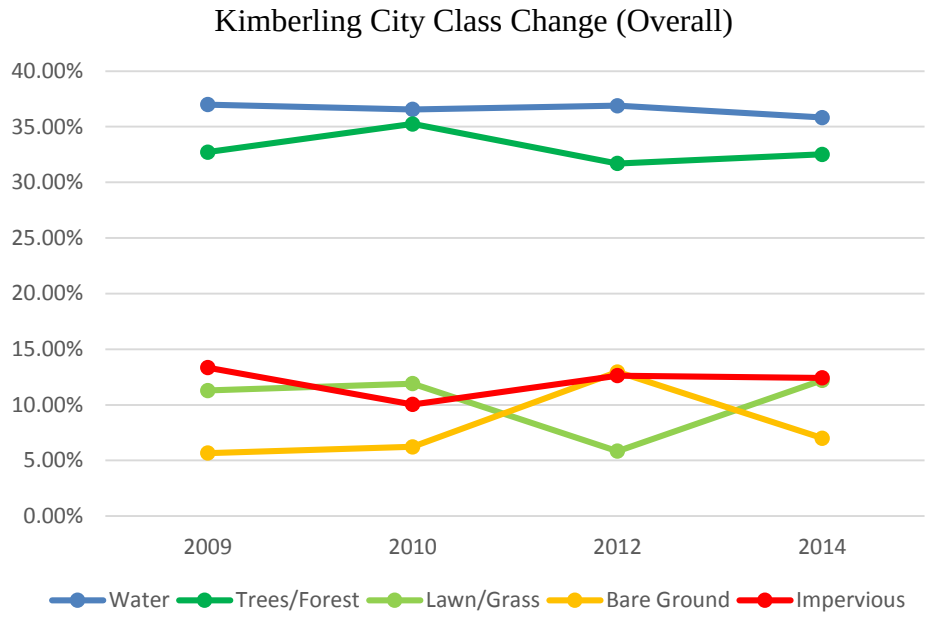

Figure 5. LULC change tendency of Kimberling City (2009-2014)

Table 12. LULC supervised classification details (m^2 and percentage) in Indian Point

	2009	2010	2012	2014
Water	9948656 (26.46%)	9459541 (25.159%)	9631455 (25.616%)	9304794 (24.751%)
Lawn/Grass	3225981 (8.58%)	4045777 (10.76%)	2990114 (7.953%)	3215821 (8.554%)
Trees/Forest	21709112 (57.738%)	21453180 (57.057%)	21347165 (56.775%)	21714226 (57.761%)
Bare Ground	475167 (1.264%)	724931 (1.928%)	1490277 (3.964%)	677038 (1.801%)
Building/Roof	786503 (2.092%)	507977 (1.351%)	852981 (2.269%)	1302633 (3.465%)
Paved Road	1233956 (3.282%)	1199324 (3.19%)	1013732 (2.696%)	1157745 (3.08%)
Parking Lot	219754 (0.584%)	208612 (0.555%)	273595 (0.728%)	209840 (0.558%)
Impervious	2240213 (5.958%)	1915913 (5.096%)	2140308 (5.693%)	2670218 (7.103%)

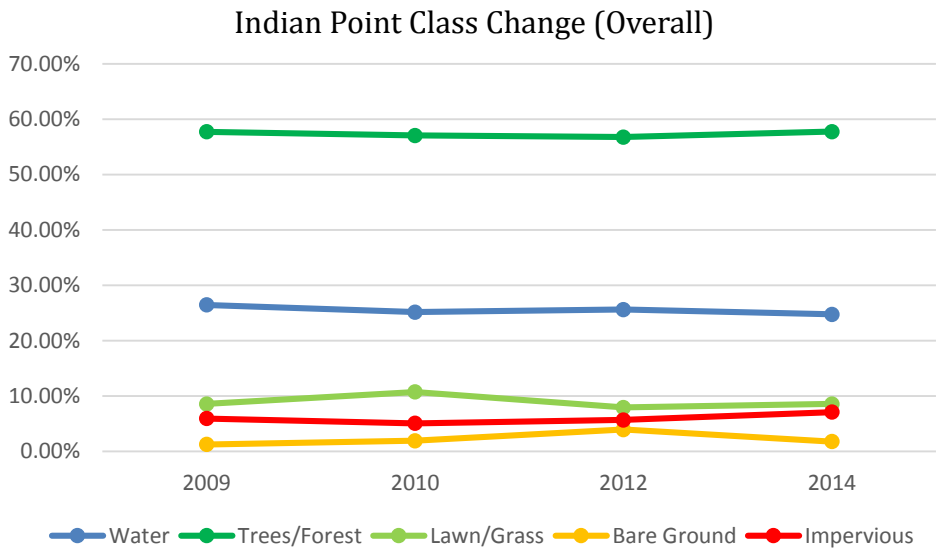

Figure 6. LULC change tendency of Indian Point (2009-2014)

Compared with the other two study areas, Indian Point seems more stable with the least fluctuation and change. Trees and forest decreased between 2009 (57.738%) and 2012, and increased back to 57.761% in the year 2014. Water body decreased by 6% during the research period. Lawns cover and impervious comprise similar percentage of land cover and converted to each other in this 5 years period.

Considering all three study areas together, some change patterns and their driving factors analysis are discussed below:

(1) The majority of the changes occurred in vegetation extension, especially trees and forests cover in the study five years. This pattern illustrates local climate, such as atmospheric temperature and rainfall, and natural environmental condition, such as soil fertility and water proportion is appropriate for vegetation growth. Also local citizens and policy makers think highly of environment protection and sustainable development.

(2) Impervious surface or artificial land use growth is not obvious. Population change is a main driving factor for land use growth, and their relationship is positive correlation. Population data (Table 15) by U.S. Census Bureau shows that in Kimberling City and Indian Point, population is decreased from 2009 to 2014 (3.0% and 28.1%). For Hollister city in Table 15, population is increased (by 10.6

%). However Table Rock Village area is only a small part in the western Hollister. Population data partly explains the low speed of urbanization process. Residential and commercial land use distribution reflects the economic development level for local regions. We could briefly conclude that economic standard in these areas have potential.

(3) The bare ground increased in middle time period (2010-2012) was converted by trees and grassland, and then converted back to vegetation (2012-2014). Regional and seasonal weather variety could lead to this phenomenon. From "from – to" change matrices, most of the converted vegetation was exchanged from bare ground, which do not raised grass or trees out of environmental and climate condition. Furthermore, daily or seasonal temperature and rainfall data could be acquired. The relationship between vegetation and bare ground land cover and climate factors could be analyzed in advanced models.

Table 13. Population change over three study areas

Location	2009	2010	2012	2014
Hollister	4051	4420	4427	4481
Kimberling City	2408	2430	2387	2335
Indian Point	718	528	524	516

Post-classification Change Detection Results (2009 to 2014)

Pixel-based "from-to" confusion matrix was generated to detect detailed changes for study areas. The land cover conversions matrices of land cover change from 2009 to 2014 of Table Rock Village, Kimberling City and Indian Point were created in Table 16, Table 17 and Table 18. In the tables, unchanged pixels are located along the major diagonal of the matrix. Hectare (ha) is an area unit equal to 10,000 m^2. Conversion values were sorted by area and listed in class scheme order. The relatively huge conversion for different land types would be described below.

Table 14. Confusion matrix of land cover change (ha) for Table Rock Village

	Water	Trees/ Forest	Lawn/ Grass	Bare Ground	Building/ Roof	Paved Road	Parking Lot	Class Total (2014)
Water	**1125.9**	2.1	0.3	1.6	1.8	1.2	3.7	1136.7
Trees/Forest	6.2	**1475.0**	*211.5*	*50.2*	10.7	*47.1*	*42.8*	1843.4
Lawn/Grass	0.9	*72.8*	**140.0**	31.9	3.9	27.6	12.5	289.7
Bare Ground	6.8	21.5	*80.3*	**56.2**	6.2	*37.5*	16.4	225.0
Building/Roof	7.4	11.2	8.5	***28.6***	**27.9**	27.0	26.9	137.7
Paved Road	7.3	16.1	14.5	18.9	4.5	**64.2**	*19.5*	145.0
Parking Lot	4.1	4.4	3.9	**12.2**	6.4	*13.7*	**21.4**	66.1
Class Total (2009)	1159.2	1604.1	459.1	199.9	61.6	218.3	143.6	0.0

Table 16 shows that in Table Rock Village between 2009 and 2014, 211.5 ha of trees and forests was converted into grass and lawns, 50.2 ha of trees and forests was converted into bare ground, 47.1 ha of trees and forests was converted to paved road, and 42.8 ha of trees was converted to parking lots. 72.8 ha of grass and lawns was converted to forests in return. 80.3 ha of bare ground was converted to grass and lawns, and 37.5 of it was converted to paved road. 28.6 ha of buildings was converted to bare ground, and this unusual changed could be caused by classification error in pervious steps.

Table 17 shows that in Kimberling City from 2009 to 2014, 53.1 ha of lawn and grass was converted to forest and trees, while 63.6 ha of forest and trees was converted back to grass land. 24 ha of bare ground was converted to trees, and 26.8 ha of it was converted to grass and lawns. 12.1 ha of buildings and 10.8 ha of parking lot was changed to bare ground land and theses conversation could be an error.

Table 15. Confusion matrix of land cover change (ha) for Kimberling City

	Water	Trees/ Forest	Lawn/ Grass	Bare Ground	Building/ Roof	Parking Lot	Paved Road	Class Total (2014)
Water	**468.4**	0.0	0.0	0.1	1.7	2.4	0.2	472.9
Trees/Forest	5.3	**326.3**	*53.1*	15.0	2.2	4.7	22.7	429.3
Lawn/Grass	3.0	*63.6*	**53.9**	14.3	2.1	4.4	20.0	161.2
Bare Ground	4.3	*24.0*	*26.8*	**16.6**	2.6	4.3	13.8	92.4
Building/Roof	2.6	4.7	5.5	***12.1***	**19.2**	8.4	15.2	67.8
Parking Lot	3.4	12.6	8.6	***10.8***	5.3	**10.7**	*17.0*	68.4
Paved Road	1.0	0.7	1.1	*5.9*	1.5	3.6	**14.1**	27.9
Class Total (2009)	488.2	431.8	149.0	74.7	34.7	38.4	103.0	0.0

Table 16. Confusion matrix of land cover change (ha) for Indian Point

	Water	Trees/ Forest	Lawn/ Grass	Bare Ground	Building/ Roof	Parking Lot	Paved Road	Class Total (2014)
Water	**916.3**	7.3	1.5	3.3	1.9	0.1	0.1	930.5
Trees/Forest	48.5	**1891.4**	*182.3*	12.0	17.9	2.4	16.9	2171.4
Lawn/Grass	2.0	*187.3*	**89.8**	11.9	9.9	2.6	18.0	321.6
Bare Ground	10.3	*18.1*	*17.7*	**8.7**	5.8	0.7	6.6	67.7
Building/Roof	14.1	***37.5***	*18.2*	8.6	**35.7**	1.1	15.1	130.3
Parking Lot	0.5	2.7	1.6	0.7	0.7	**12.6**	2.2	21.0
Paved Road	3.1	***26.0***	11.3	2.4	6.2	2.5	**64.4**	115.8
Class Total (2009)	994.9	2170.5	322.5	47.5	78.6	22.0	123.4	0.0

Table 18 shows that in Indian Point between 2009 and 2014, 182.3 ha of lawn and grass was turned to forest and trees, while 187.3 ha of forest and trees was converted back to grass land. 18.1 ha trees cover and 17.7 grass covered land were converted from bare ground. 37.5 ha of buildings and 26.0 ha of paved road was converted into trees and forests.

There are many unusual changes in detection judged by author's common sense. So a visualization detection of bitemporal images especially for unusual buildings conversions are conducted to compare the relationship with post-classification confusion matrices. The post-classification results enable tracking the trajectory of each pixel between the two time steps of observation. Two examples of visualization detection results are showing in Figure 7 and Figure 8. Figure 7 shows a clear group of apartments completed in Indian Point, and Figure 8 displays there is apparent obvious change in residential areas of Kimberling City. Three new construction regions are detected and located in Indian Point and Table Rock Village, while there is no urbanization evidence in Kimberling City during the recent five years. This straightforward visualization comparison states a different result from post-classification confusion matrix in impervious surface land cover.

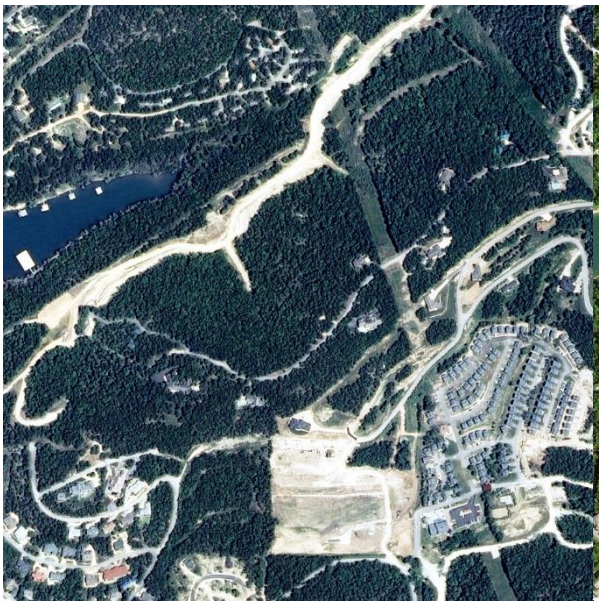

Aerial Photo for Table Rock Village Residential Area (2009)

Aerial Photo for Table Rock Village Residential Area (2014)

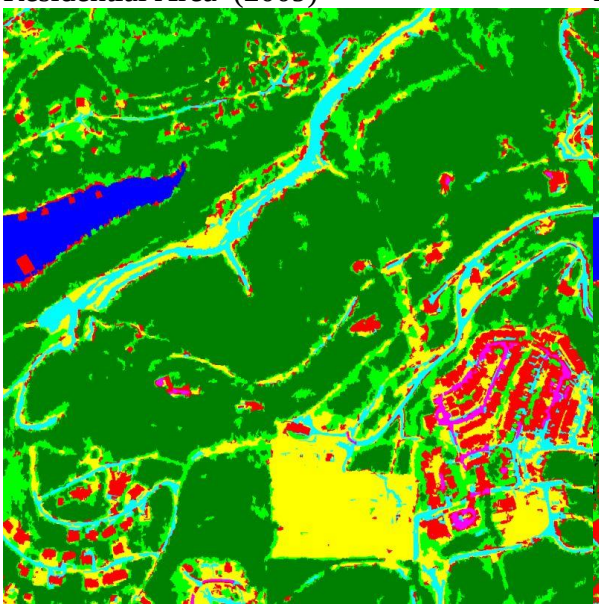

Classification Results for Table Rock Village Residential Area (2009)

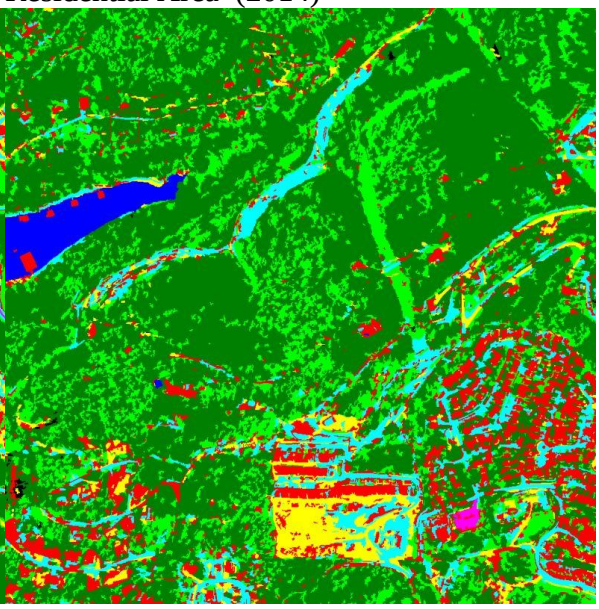

Classification Results for Table Rock Village Residential Area (2014)

Figure 7. Visualization of a changed residential area in Indian Point

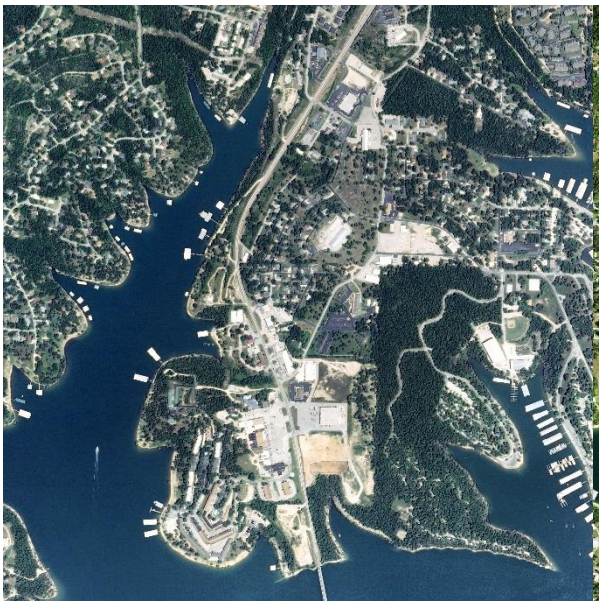

Aerial Photo for Kimberling City Residential Area (2009)

Aerial Photo for Kimberling City Residential Area (2014)

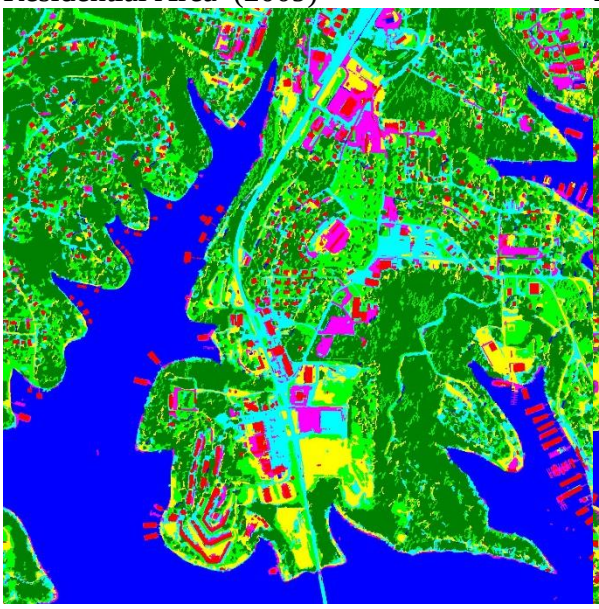

Classification Results for Kimberling City Residential Area (2009)

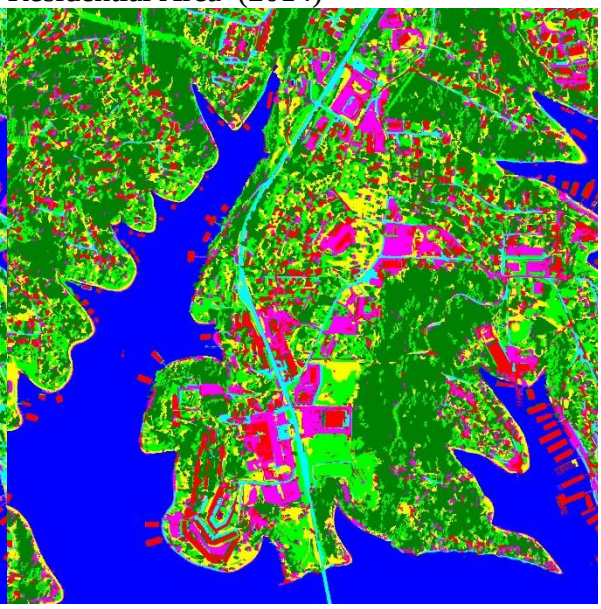

Classification Results for Kimberling City Residential Area (2014)

Figure 8. Visualization of a changed residential area in Kimberling City

The error changes are most likely related with omission and commission errors in the NAIP object-based classification map. From the classification error matrix in Table 18, the misclassification for buildings, parking lots and bare ground did happen.

Registration errors and edge effects can also influence the errors appearing in the determination of change or no change. In this study, geometric rectification of aerial imagery was undertaken by NAIP before classification, there are obvious one meter to three meter's image distortions between initial year 2009 and ending year 2014 regionally. Edge error could be caused in image segmentation. Although the spatial registration error is recognized hardly to avoid, this is still of a significant concern requiring NAIP technician to improve.

CONCLUSION

The results demonstrate that NAIP classifications can be used to produce accurate land cover classification map and statistics. Compared with other pixel-based and object-based approaches (rule-based decision tree, CART, nearest neighbor classifier, Bayes classifier, maximum likelihood classifier), random tree is verified to be the most optimal classification method for one meter resolution NAIP aerial photo without auxiliary data in terms of efficiency and accuracy. NAIP imagery could be utilized for quick classification, but the possible shadows disaster and light impact could restrict the change detection result, especially for impervious surface. Overall patterns and dynamic tendencies of LULC in the Table Rock Lake regions were detected by: (1) classifying the area amount of land cover in Table Rock Village, Kimberling City and Indian Point and during four periods from 2009 to 2014; (2) comparing the results of derived statistics for seven classification types and (3) analyzing the LULC change patterns and relative driving forces, such as population variety. We found (1) the majority of the changes occurred in vegetation extension, especially trees and forests cover; (2) Impervious surface or artificial land use growth is not obvious; and (3) vegetation and bare ground exchanged to each other by seasonal period in different years. Although the Table Rock Lake Region economic development is in a relatively slow speed, the potential opportunity is great for its healthy environmental condition and geographical location.

Future research can be done in straightforward object-based post-classification change detection techniques, and acquiring relevant auxiliary data. The auxiliary information such as height data (Lidar, digital elevation model) could possibly improve

the classification accuracy for impervious surface land type. Object-based post-classification change detection is a new method for high resolution images that could avoid the edge error and registration errors. Finally, the improved procedure of classification and LULC change detection for this study could be widely applied in different landscapes at the region level in the United States and the rest of the world.

REFERENCES

Abd El-Kawy, O. R., Rød, J. K., Ismail, H. A., & Suliman, A. S. (2011). Land use and land cover change detection in the western Nile delta of Egypt using remote sensing data. *Applied Geography, 31*(2), 483-494.

Bandyopadhyay, S., & Pal, S. K. (2001). Pixel classification using variable string genetic algorithms with chromosome differentiation. *IEEE Transactions on Geoscience Remote Sensing, 39*(2), 303–308.

Banko, G. (1998). *A review of assessing the accuracy of classifications of remotely sensed data and of methods including remote sensing data in forest inventory* (No. ir98081).

Bennett, K. P., & Demiriz, A. (1998). Semi-supervised support vector machines. *Advances in Neural Information Processing Systems, 10*, 368–374.

Benz, U. C., Hofmann, P., Willhauck, G., Lingenfelder, I., & Heynen, M. (2004). Multi-resolution, object-oriented fuzzy analysis of remote sensing data for GIS-ready information. *ISPRS Journal of photogrammetry and remote sensing, 58*(3), 239-258.

Brown, L. G. (1992). A survey of image registration techniques. *ACM computing surveys (CSUR), 24*(4), 325-376.

Byrne, G. F., Crapper, P. F., & Mayo, K. K. (1980). Monitoring land cover change by principal component analysis of multitemporal Landsat data. *Remote Sensing of Environment, 10*, 175-184.

Canty, M. J., & Nielsen, A. A. (2006). Visualization and unsupervised classification of changes in multispectral satellite imagery. *International Journal of Remote Sensing, 27*(18), 3961–3975.

Chen, J., Gong, P., He, C., Pu, R., & Shi, P. (2003). Land-use/land-cover change detection using improved change-vector analysis. *Photogrammetric engineering and remote sensing, 69*(4), 369-379.

Cohen, W. B., Yang, Z., & Kennedy, R. (2010). Detecting trends in forest disturbance and recovery using yearly Landsat time series: 2. TimeSync—Tools for calibration and validation. *Remote Sensing of Environment, 114*(12), 2911-2924.

Dai, X., & Khorram, S. (1998). The effects of image misregistration on the accuracy of remotely sensed change detection. *Geoscience and Remote Sensing, IEEE Transactions on, 36*(5), 1566-1577.

Davies, K. W., Petersen, S. L., Johnson, D. D., Davis, D. B., Madsen, M. D., Zvirzdin, D. L., & Bates, J. D. (2010). Estimating juniper cover from National Agriculture Imagery Program (NAIP) imagery and evaluating relationships between potential cover and environmental variables.*Rangeland Ecology & Management*, *63*(6), 630-637.

Desclée, B., Bogaert, P., & Defourny, P. (2006). Forest change detection by statistical object-based method. *Remote Sensing of Environment*, *102*(1), 1-11.

Dinger, J. S., Zourarakis, D. P., & Currens, J. C. (2007). Spectral enhancement and automated extraction of potential sinkhole features from NAIP imagery—initial investigations. *Journal of Environmental Informatics*, *10*(1), 22-29.

Eklundh, L., & Singh, A. (1993). A comparative analysis of standardized and unstandardized Principal Components Analysis in remote sensing. *International Journal of Remote Sensing*, *14*(7), 1359-1370.

Fuller, D. O. (1998). Trends in NDVI time series and their relation to rangeland and crop production in Senegal, 1987-1993. *International Journal of Remote Sensing*, *19*(10), 2013-2018.

Hansen, M. C., DeFries, R. S., Townshend, J. R., & Sohlberg, R. (2000). Global land cover classification at 1 km spatial resolution using a classification tree approach. *International journal of remote sensing*, *21*(6-7), 1331-1364.

Hughes, G. F. (1968). On the mean accuracy of statistical pattern recognizers. *IEEE Transactions on Information Theory*, *14*(1), 55–63.

Gao, B. C. (1996). NDWI— A normalized difference water index for remote sensing of vegetation liquid water from space. *Remote sensing of environment*, *58*(3), 257-266.

Gianinetto, M., & Villa, P. (2011). Mapping hurricane Katrina's widespread destruction in New Orleans using multisensor data and the normalized difference change detection (NDCD) technique. *International Journal of Remote Sensing, 32(7),* 1961–1982.

Huang, C., Goward, S. N., Masek, J. G., Thomas, N., Zhu, Z., & Vogelmann, J. E. (2010). An automated approach for reconstructing recent forest disturbance history using dense Landsat time series stacks. *Remote Sensing of Environment*, *114*(1), 183-198.

Ingebritsen, S. E., & Lyon, R. J. P. (1985). Principal components analysis of multitemporal image pairs. *International Journal of Remote Sensing, 6(5),* 687–696.

Jensen, R. J. (2007). Image Enhancement. In R. J. Jensen, *Introductory Digital Image Processing* (255-335). New Jersey: Pearson.

Jun, G., & Ghosh, J. (2011). Spatially adaptive semi-supervised learning with Gaussian processes for Hyperspectral data analysis. *Statistical Analysis and Data Mining: The ASA Data Science Journal, 4*(4), 358-371.

Jun, G., Vatsavai, R. R., & Ghosh, J. (2009, December). Spatially adaptive classification and active learning of multispectral data with Gaussian processes. In *Data Mining Workshops, 2009. ICDMW'09. IEEE International Conference on* (pp. 597-603). IEEE.

Li, X., & Shao, G. (2014). Object-based land-cover mapping with high resolution aerial photography at a county scale in midwestern USA. *Remote Sensing*, *6*(11), 11372-11390.

Liu, J., & Gao, M. (2008, December). An Unsupervised Classification Scheme Using PDDP Method for Network Intrusion Detection. In *Intelligent Information Technology Application, 2008. IITA'08. Second International Symposium on* (Vol. 3, pp. 658-662). IEEE.

Liu, X., Li, X., Liu, L., & He, J. (2008). An innovative method to classify remote sensing image using ant colony optimization. *IEEE Transactions on Geoscience Remote Sensing, 46*(12), 4198–4208.

Longley, P. A., Goodchild, M., Maguire, D. J., & Rhind, D. W. (2011). *Geographic Information Systems and Science: Systems, science, and study*. Southern Gate, Chichester, West Sussex, England: Wiley.

Lu, D., Mausel, P., Brondizio, E., & Moran, E. (2004). Change detection techniques. *International journal of remote sensing*, *25*(12), 2365-2401.

Lunetta, R. S., Knight, J. F., Ediriwickrema, J., Lyon, J. G., & Worthy, L. D. (2006). Land-cover change detection using multi-temporal MODIS NDVI data. *Remote sensing of environment*, *105*(2), 142-154.

Nielsen, A. A., & Conradsen, K. (1997). Multivariate alteration detection (MAD) in multispectral, bi-temporal image data: A new approach to change detection studies. *IMM Technical Report*, *11*.

Maxwell, A. E., Strager, M. P., Warner, T. A., Zégre, N. P., & Yuill, C. B. (2014). Comparison of NAIP orthophotography and RapidEye satellite imagery for

mapping of mining and mine reclamation. *GIScience & Remote Sensing, 51*(3), 301-320.

Miao, X., Xie, H., Ackley, S. F., Perovich, D. K., & Ke, C. (2015). Object-based detection of Arctic sea ice and melt ponds using high spatial resolution aerial photographs. *Cold Regions Science and Technology, 119*, 211-222.

Mitra, P., Shankar, B. U., & Pal, S. K. (2004). Segmentation of multispectral remote sensing images usingactive support vector machines. *Pattern Recognition Letters, 25*(9),1067–1074.

Patra, S., Ghosh, S., & Ghosh, A. (2007). Semi-supervised learning with multilayer perceptron for detecting changes of Remote Sensing images. In A., Ghosh, *Pattern Recognition and Machine Intelligence* (161-168). Kolkata, India: Springer Berlin Heidelberg.

Qiu, X., Wu, S. S., & Miao, X. (2014). Incorporating road and parcel data for object-based classification of detailed urban land covers from NAIP images. *GIScience & Remote Sensing, 51*(5), 498-520.

Rashed, T., Weeks, J. R., Stow, D., & Fugate, D. (2005). Measuring temporal compositions of urban morphology through spectral mixture analysis: toward a soft approach to change analysis in crowded cities. *International Journal of Remote Sensing, 26*(4), 699-718.

Rozenstein, O., & Karnieli, A. (2011). Comparison of methods for land-use classification incorporating remote sensing and GIS inputs, *Applied Geography, 31*, 533-544.

Samaniego, L., Bárdossy, A., & Schulz, K. (2008). Supervised classification of remotely sensed imagery using a modified-NN technique. *Geoscience and Remote Sensing, IEEE Transactions on, 46*(7), 2112-2125.

Singh, A. (1989). Review article digital change detection techniques using remotely sensed data. *International Journal of Remote Sensing, 10*(6), 989–1003.

Stow, D. (2010). Geographic object-based image change analysis. In *Handbook of applied spatial analysis* (pp. 565-582). Berlin: Springer Berlin Heidelberg.

Toll, D. L., Royal, I. A., & Davis, J. B. (1980). Urban area up-date procedures using Landsat data: *Proceedings of the Fall Technical Meeting of the American Society of Photogrammetry*. Niagara Falls, Canada: ASP.

Townshend, J. R., Justice, C. O., Gurney, C., & McManus, J. (1992). The impact of misregistration on change detection. *Geoscience and Remote Sensing, IEEE Transactions on, 30*(5), 1054-1060.

Tuia, D., Ratle, F., Pacifici, F., Kanevski, M. F., & Emery, W. J. (2009). Active learning methods for remote sensing image classification. *IEEE Transactions on Geoscience and Remote Sensing, 47*(7), 2218-2232.

U.S. Census Bureau. (2010). Missouri Population: Stone County. Retrieved December, 2015, from http://censusviewer.com/cities/MO.

Van, Niel, T., McVicar, T., & Datt, B. (2005). On the relationship between training sample size and data dimensionality: Monte Carlo analysis of broadband multi-temporal classification. *Remote Sensing. Environment, 98*, 468–480.

Van Oort, P. A. J. (2007). Interpreting the change detection error matrix. *Remote Sensing of Environment*, *108*(1), 1-8.

Xiuwan, C. (2002). Using remote sensing and GIS to analyse land cover change and its impacts on regional sustainable development. *International Journal of Remote Sensing*, *23*(1), 107-124.

Yuan, D., Elvidge, C. D., & Lunetta, R. S. (1998). Survey of multispectral methods for land cover change analysis. Remote sensing change detection: Environmental monitoring methods and applications (pp. 21 – 39). Michigan: Ann Arbor Press.

APPENDICES

Appendix A. LULC Classification Results for Six Classification Methods

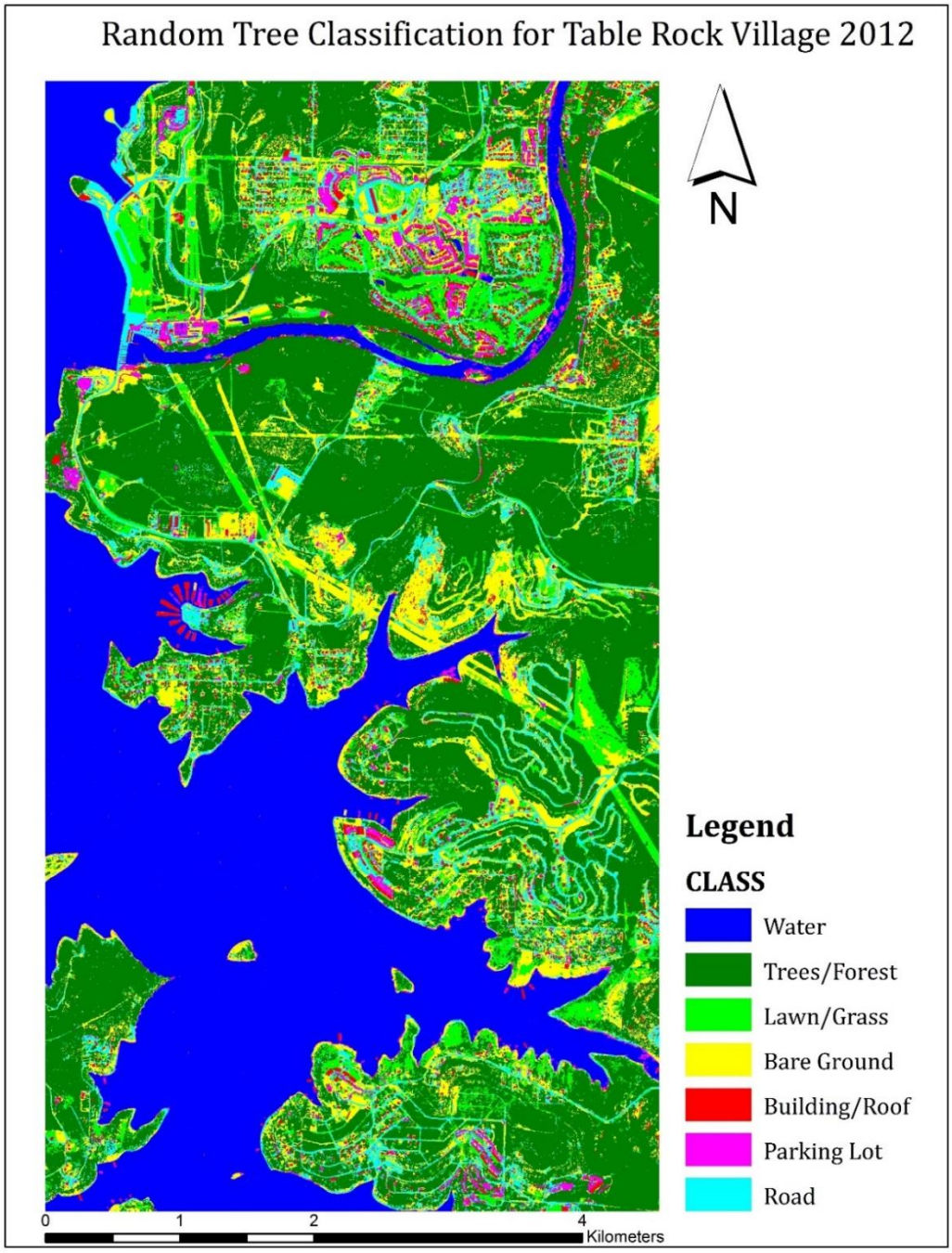

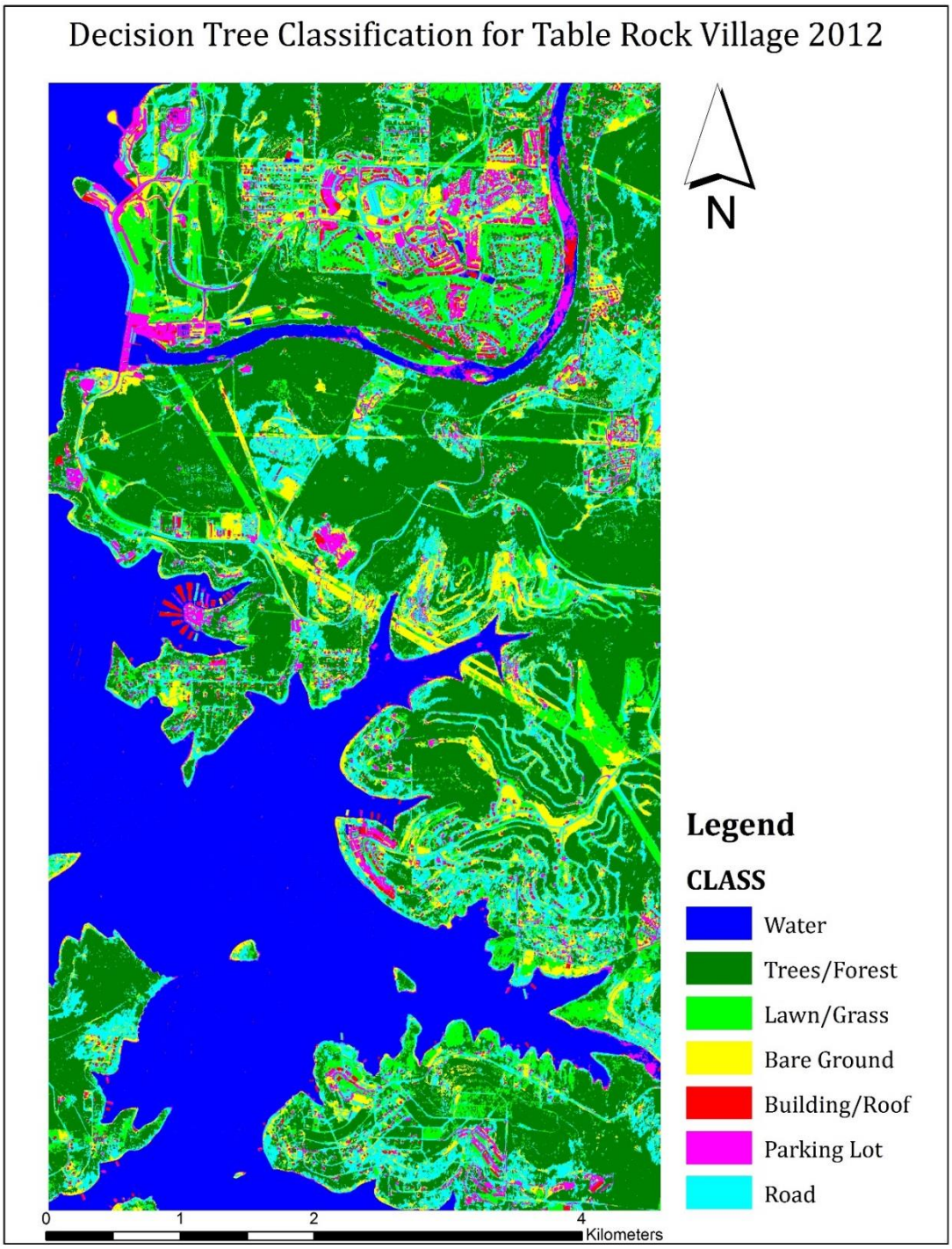
Decision Tree Classification for Table Rock Village 2012
N
Legend
CLASS
Water
Trees/Forest
Lawn/Grass
Bare Ground
Building/Roof
Parking Lot
Road
0
1
2
4
Kilometers

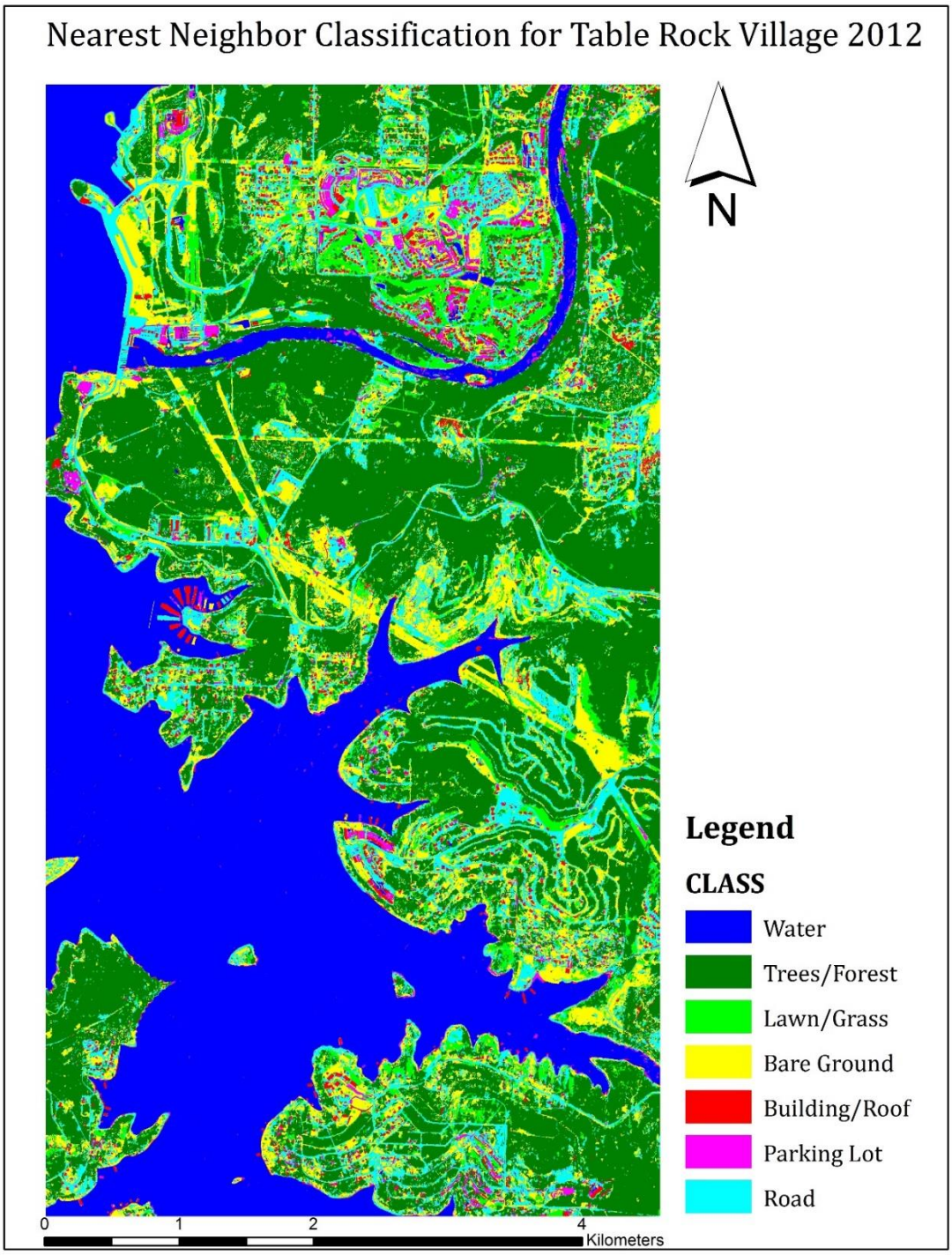
Nearest Neighbor Classification for Table Rock Village 2012
N
Legend
CLASS
Water
Trees/Forest
Lawn/Grass
Bare Ground
Building/Roof
Parking Lot
Road
0
1
2
4
Kilometers

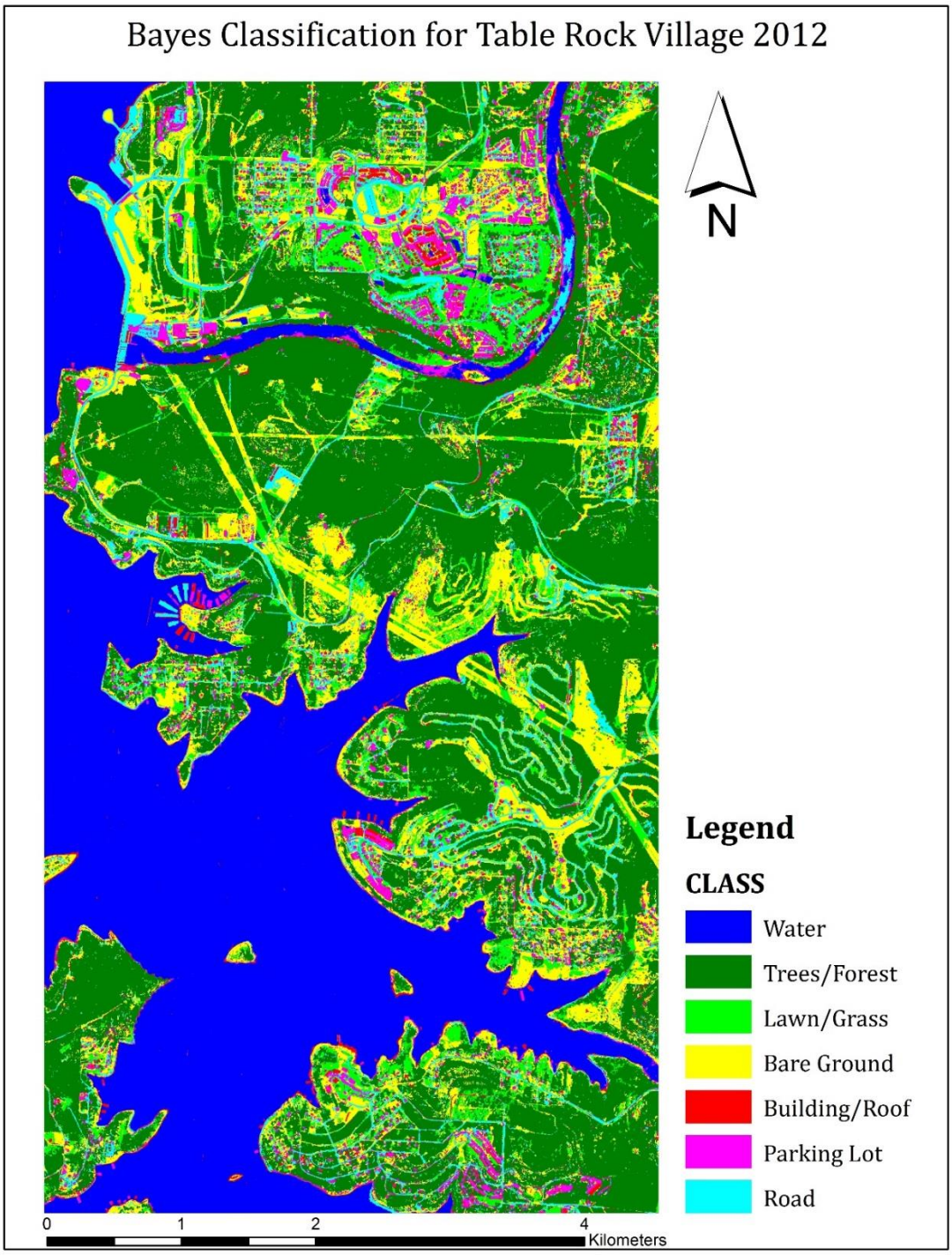
Bayes Classification for Table Rock Village 2012
N
Legend
CLASS
Water
Trees/Forest
Lawn/Grass
Bare Ground
Building/Roof
Parking Lot
Road
0
1
2
4
Kilometers

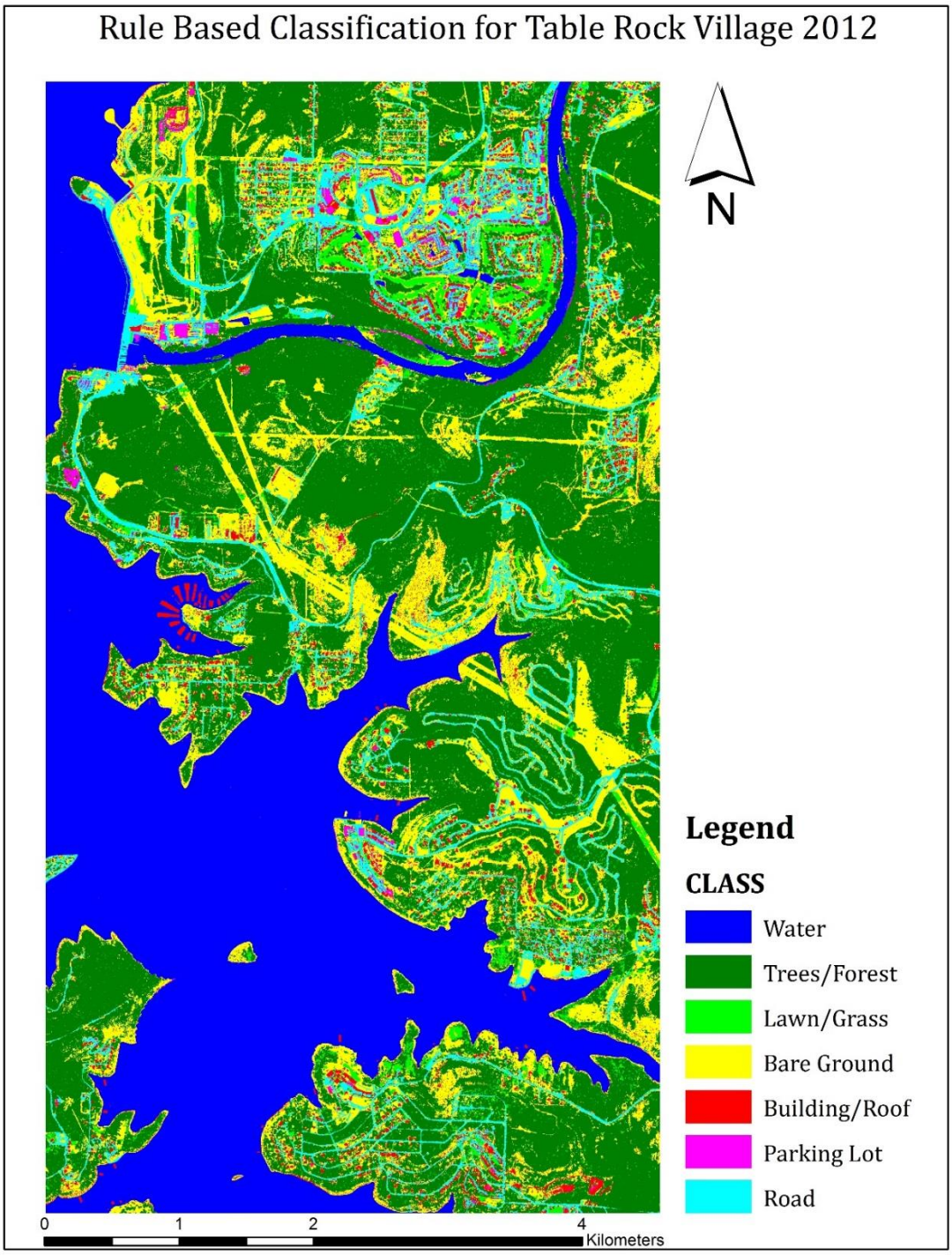
Rule Based Classification for Table Rock Village 2012
N
Legend
CLASS
Water
Trees/Forest
Lawn/Grass
Bare Ground
Building/Roof
Parking Lot
Road
0
1
2
4
Kilometers

Appendix B. Accuracy Assessment Confusion Matrices in Percentage for Six Classification Methods

Confusion matrix for random tree (Table Rock Village 2012)

Class	Water	Trees/ Forest	Lawn/ Grass	Bare Ground	Building/ Roof	Parking Lots	Road	Total
Water	90.71	0	0	0	0	4.3	0	28
Trees/Forest	0	93.69	0.54	0	0.02	0	0.02	5.5
Lawn/Grass	0	3.28	98.65	6.61	0.37	0	0.03	6.74
Bare Ground	0	0.86	0.73	83.11	6.84	0.36	0.85	5.57
Building/Roof	4.62	0.04	0	1.94	78.3	7.11	2.41	19.47
Parking Lots	4.67	0	0.02	0.46	13.24	80.8	1.39	16.66
Road	0	2.13	0.06	7.88	1.24	7.41	95.3	18.06
Total	100	100	100	100	100	100	100	100

Confusion matrix for decision tree (Table Rock Village 2012)

Class	Water	Trees/ Forest	Lawn/ Grass	Bare Ground	Building/ Roof	Parking Lots	Road	Total
Water	91.61	0	0	0	1.36	12.09	0	29.74
Trees/Forest	0	89.16	0.41	0	0	0	0.03	5.23
Lawn/Grass	0	5.39	98.07	6.63	0.01	0.04	0.12	6.77
Bare Ground	0	0	0.05	68.8	3.52	0.54	3.4	4.58
Building/Roof	4.28	0	0	1.05	70.84	6.94	1.83	17.62
Parking Lots	4.11	0	0.02	11.38	18.71	76.24	10.93	19.08
Road	0.01	5.45	1.45	12.14	5.56	4.14	83.7	16.99
Total	100	100	100	100	100	100	100	100

Confusion matrix for nearest-neighbor classifier (Table Rock Village 2012)

Class	Water	Trees/ Forest	Lawn/ Grass	Bare Ground	Building/ Roof	Parking Lots	Road	Total
Water	98.65	0	0	0	0.75	2.36	0	30.26
Trees/Forest	0	88.71	4.03	0.02	0.01	0	0.06	5.44
Lawn/Grass	0	5.86	76.64	3.8	0	0.02	0.04	5.31
Bare Ground	0	2.63	16.23	74.7	16.8	0.36	9.86	10.8
Building/Roof	0.61	0.03	0	1.76	67.97	10.63	0.87	16.34
Parking Lots	0.74	0	0.02	0	10.93	72.33	2.82	16.34
Road	0	2.77	3.08	19.72	3.55	14.29	86.35	18.84
Total	100	100	100	100	100	100	100	100

Confusion matrix for Bayes classifier (Table Rock Village 2012)

Class	Water	Trees/ Forest	Lawn/ Grass	Bare Ground	Building/ Roof	Parking Lots	Road	Total
Water	92.52	0	0	0	0	7.76	0	29.07
Trees/Forest	0	90.91	0.54	0	0.01	0	0	5.34
Lawn/Grass	0	8.56	81.8	3.32	0.06	0.02	0.01	5.78
Bare Ground	0	0.03	9.86	87.6	11.38	0.07	15.39	9.68
Building/Roof	0.52	0	0.02	1.83	29.81	3.79	4.06	7.79
Parking Lots	5.31	0	0.02	0.68	47.28	77.84	1.74	23.64
Road	1.65	0.5	7.76	6.56	11.46	10.51	78.8	18.7
Total	100	100	100	100	100	100	100	100

Confusion matrix for semi-automated rule-based (Table Rock Village 2012)

Class	Water	Trees/ Forest	Lawn/ Grass	Bare Ground	Building/ Roof	Parking Lots	Road	Total
Water	99.82	0	0	0.3	0.17	0	0	30.15
Trees/Forest	0	95.68	5.75	0	0.01	0.11	0.04	5.96
Lawn/Grass	0	3.01	85.25	0	0	0	0	5.5
Bare Ground	0	1.31	9	88.76	10.12	5.67	7.43	8.99
Building/Roof	0	0	0	1.76	70.21	11.87	0.84	16.81
Parking Lots	0.18	0	0	0.08	6.67	55.56	0.18	9.88
Road	0	0	0	9.09	12.82	26.79	91.51	22.71
Total	100	100	100	100	100	100	100	100

Confusion matrix for pixel-based maximum likelihood (Table Rock Village 2012)

Class	Water	Trees/ Forest	Lawn/ Grass	Bare Ground	Building/ Roof	Parking Lots	Road	Total
Water	78.66	0	0	0	0.16	4.45	0	24.43
Trees/Forest	0	92.95	3.48	0	0	0	0	5.64
Lawn/Grass	0	6.91	95.12	2.21	0.38	0.3	0.25	6.61
Bare Ground	0	0.05	1.39	72.22	12.96	1.79	7.2	7.65
Building/Roof	4.41	0.09	0.01	3.02	31.67	8.54	2.76	9.91
Parking Lots	12.87	0	0	0	10.57	70.97	0.8	16.96
Road	4.07	0	0	22.55	44.26	13.94	88.98	28.82
Total	100	100	100	100	100	100	100	100

Appendix C. LULC Classification Results for Table Rock Village, Kimberling City and Indian Point in 2009, 2010, 2012 and 2014

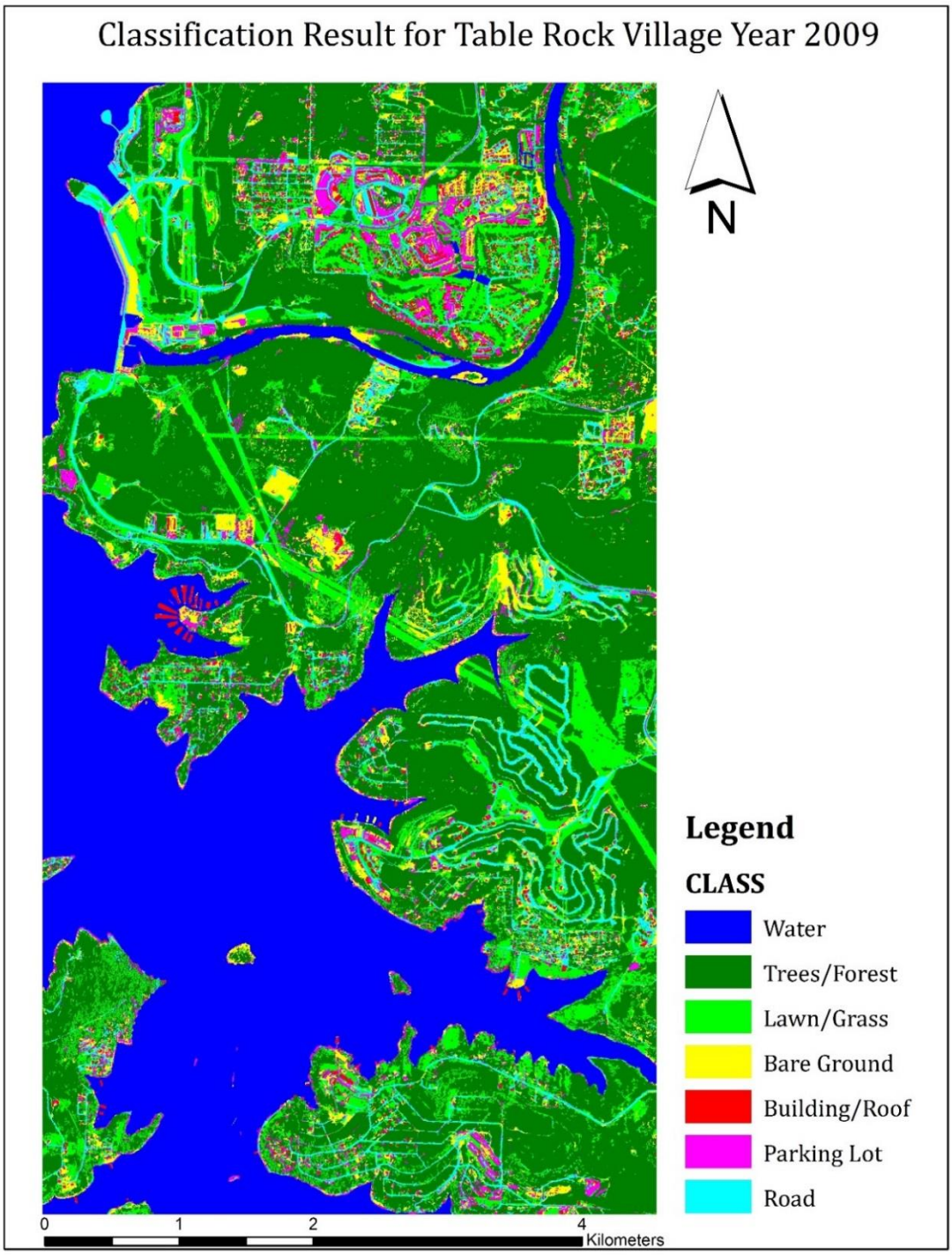

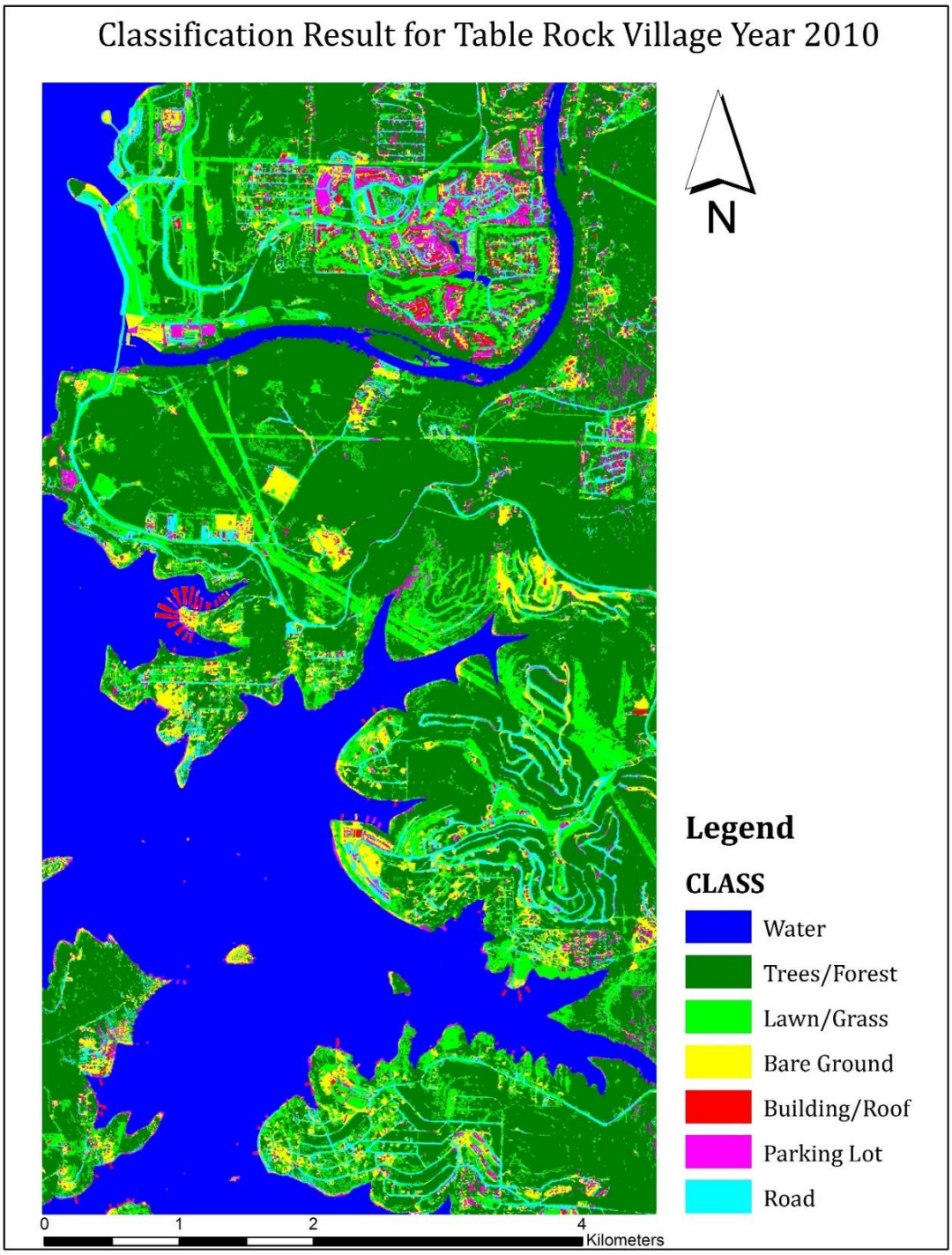
Classification Result for Table Rock Village Year 2010
N
Legend
CLASS
Water
Trees/Forest
Lawn/Grass
Bare Ground
Building/Roof
Parking Lot
Road
0
1
2
4
Kilometers

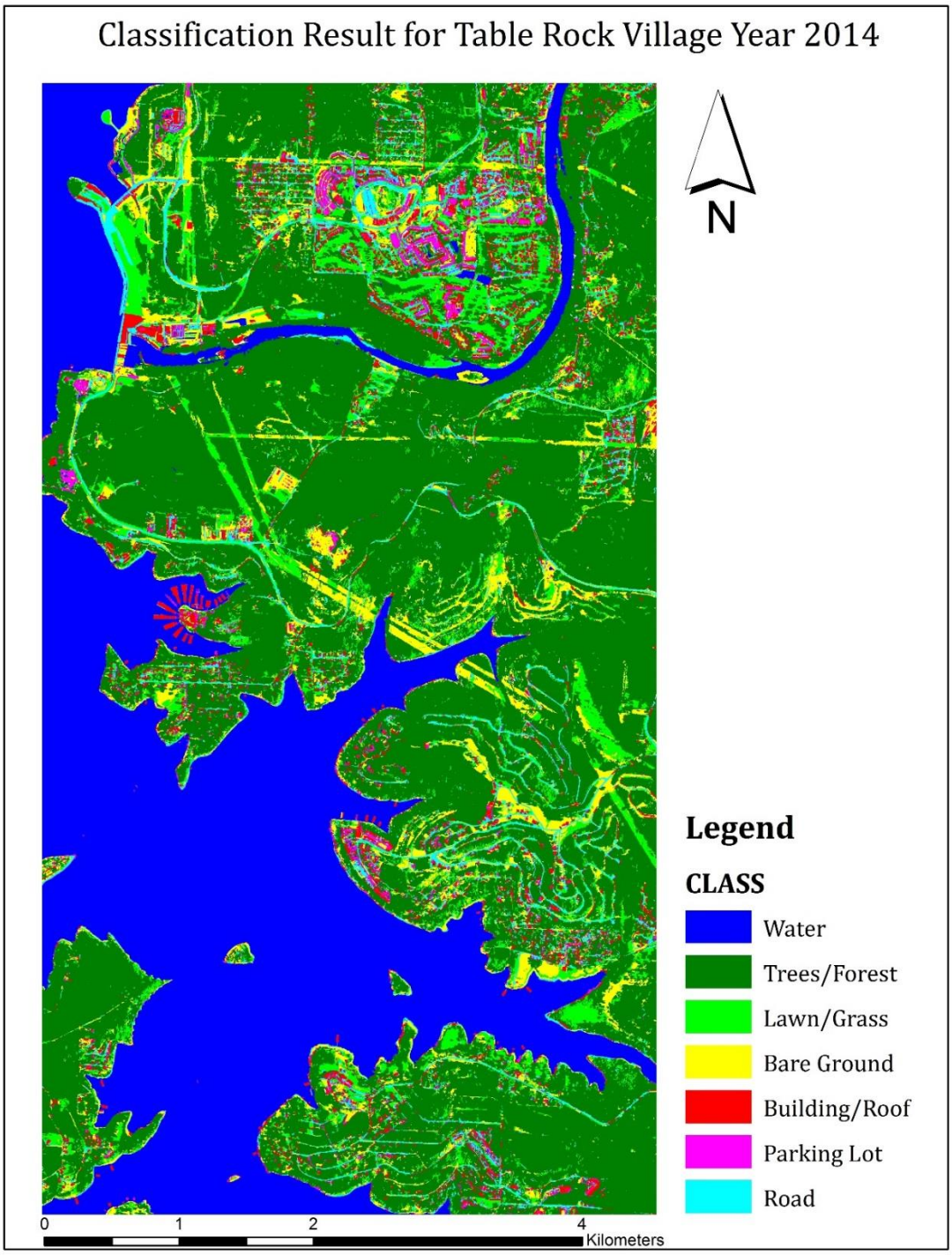
Classification Result for Table Rock Village Year 2014
N
Legend
CLASS
Water
Trees/Forest
Lawn/Grass
Bare Ground
Building/Roof
Parking Lot
Road
0
1
2
4
Kilometers

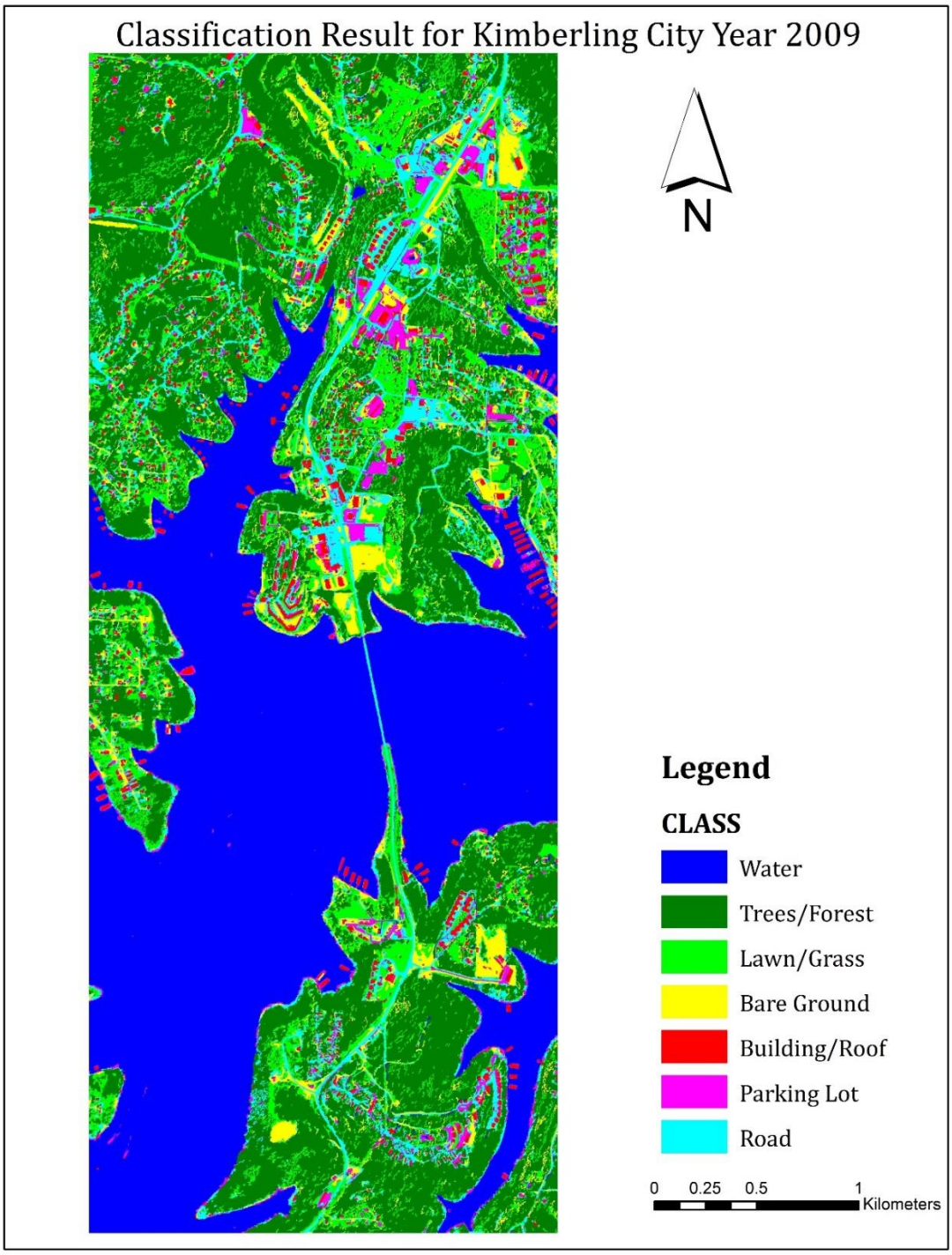
Classification Result for Kimberling City Year 2009
N
Legend
CLASS
Water
Trees/Forest
Lawn/Grass
Bare Ground
Building/Roof
Parking Lot
Road
0 0.25 0.5 1
Kilometers

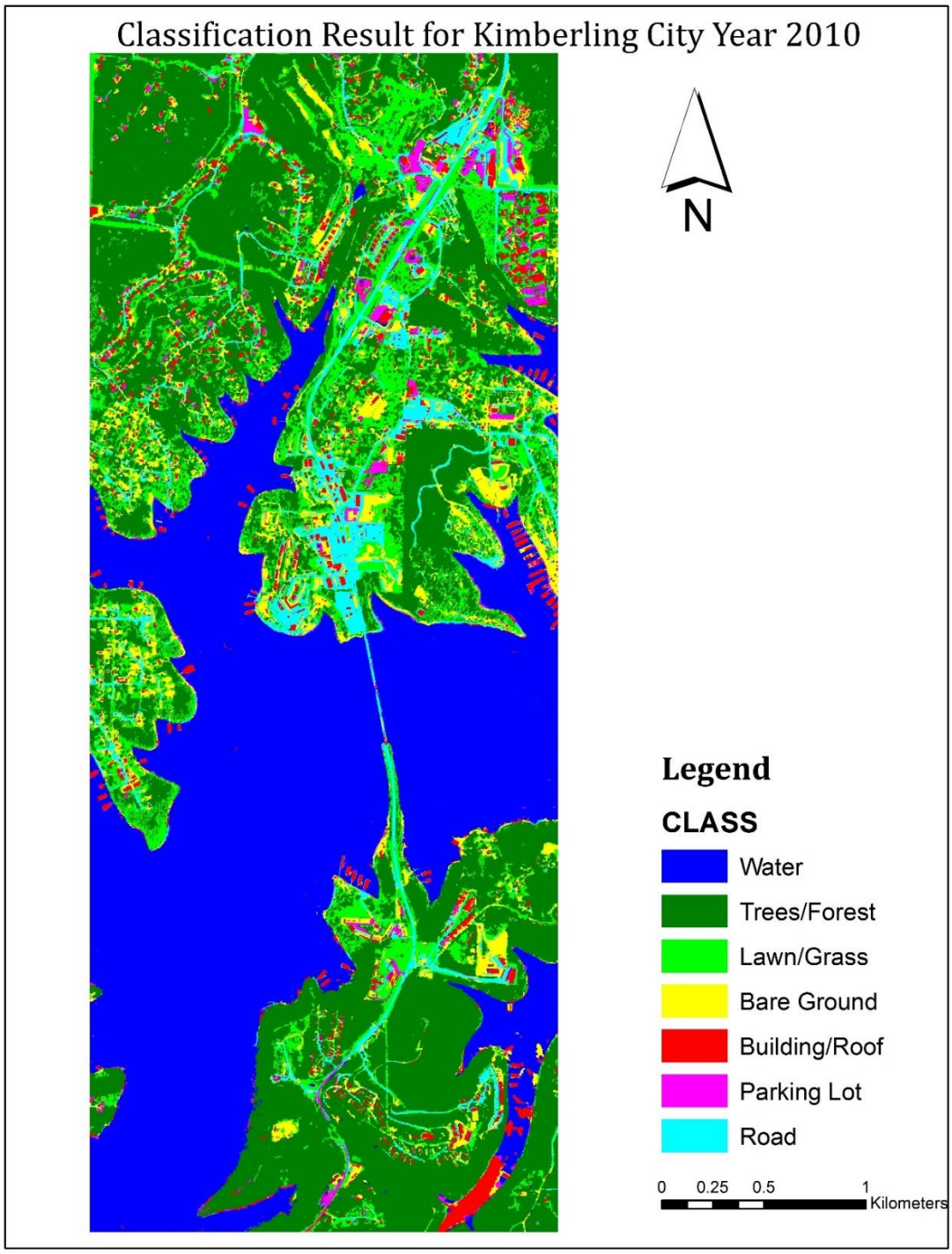
Classification Result for Kimberling City Year 2010
N
Legend
CLASS
Water
Trees/Forest
Lawn/Grass
Bare Ground
Building/Roof
Parking Lot
Road
0 0.25 0.5 1
Kilometers

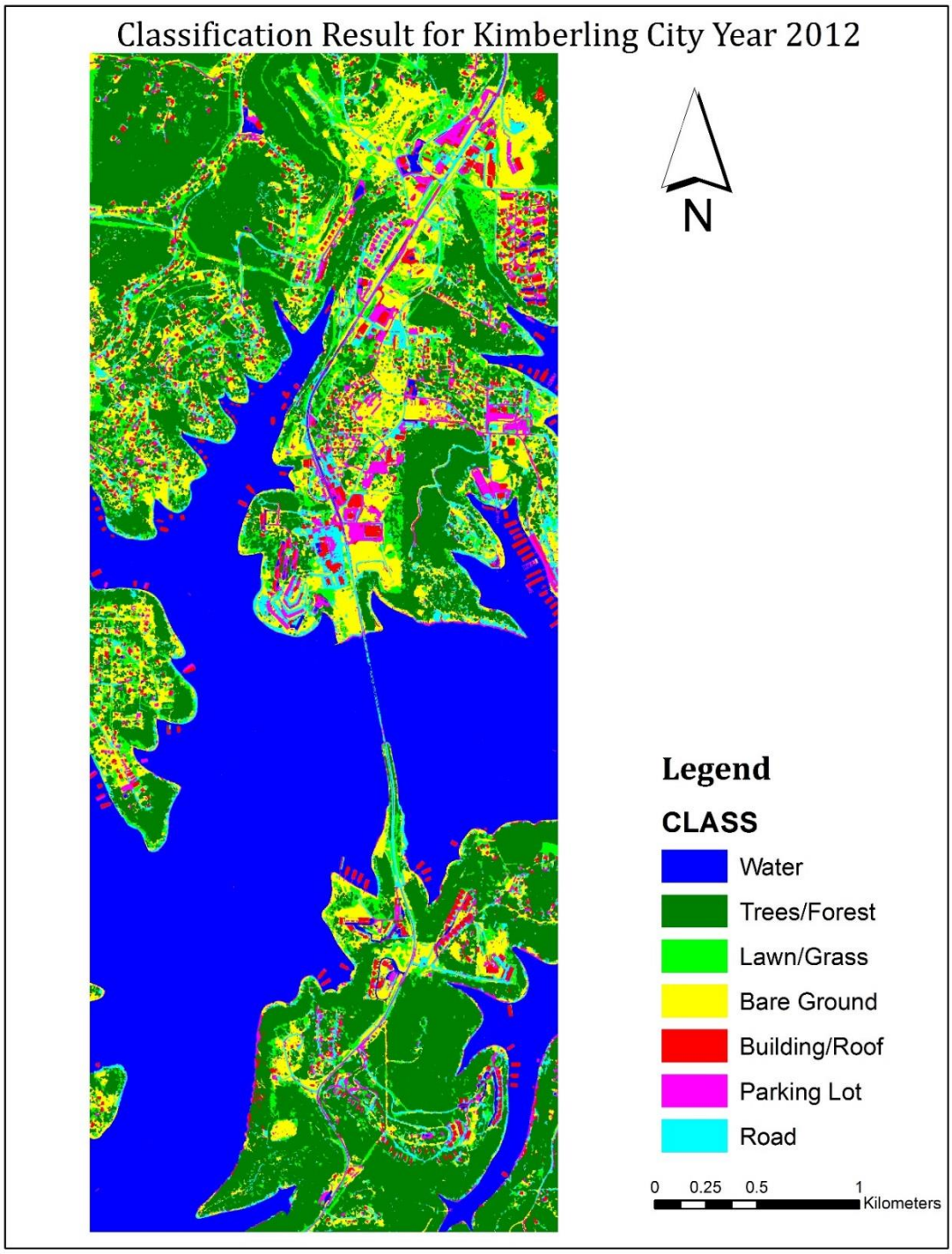
Classification Result for Kimberling City Year 2012
N
Legend
CLASS
Water
Trees/Forest
Lawn/Grass
Bare Ground
Building/Roof
Parking Lot
Road
0 0.25 0.5 1
Kilometers

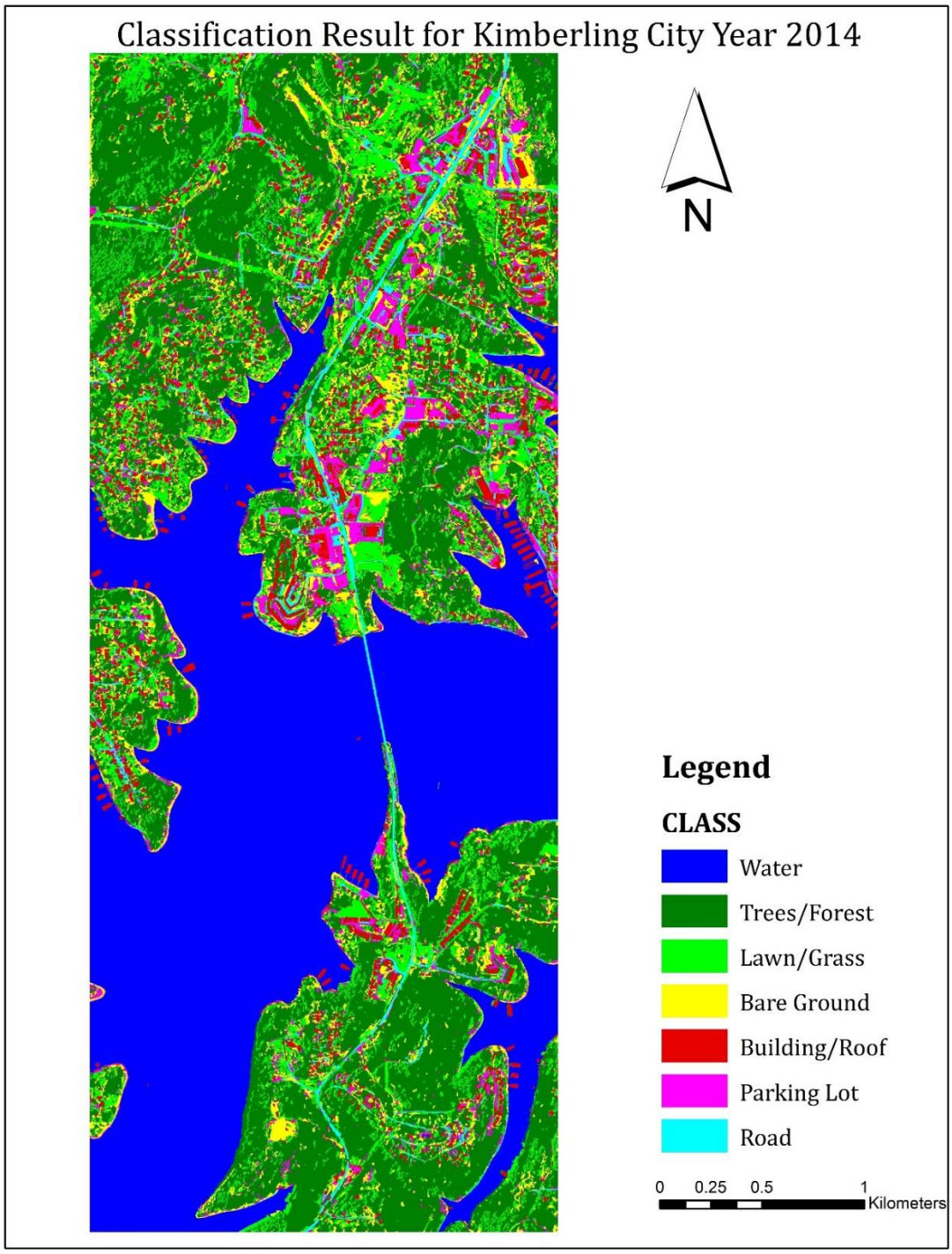
Classification Result for Kimberling City Year 2014
N
Legend
CLASS
Water
Trees/Forest
Lawn/Grass
Bare Ground
Building/Roof
Parking Lot
Road
0 0.25 0.5 1
Kilometers

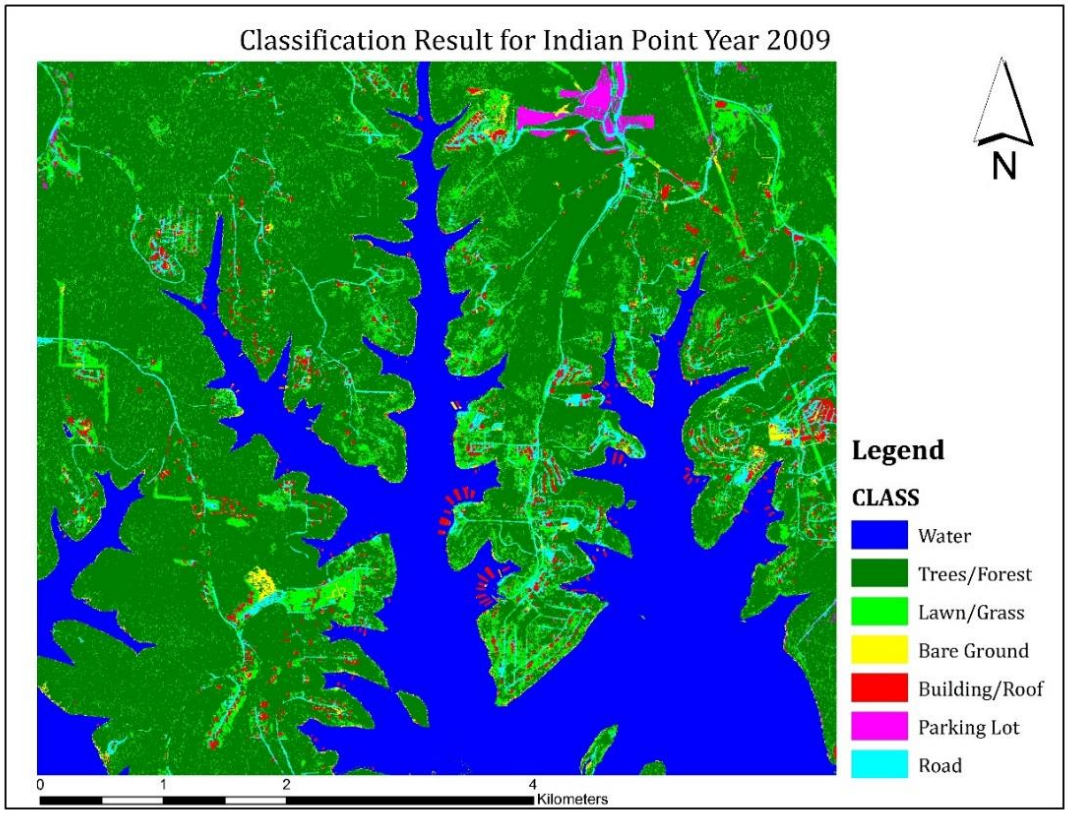
Classification Result for Indian Point Year 2009
N
Legend
CLASS
Water
Trees/Forest
Lawn/Grass
Bare Ground
Building/Roof
Parking Lot
Road
0
1
2
4
Kilometers

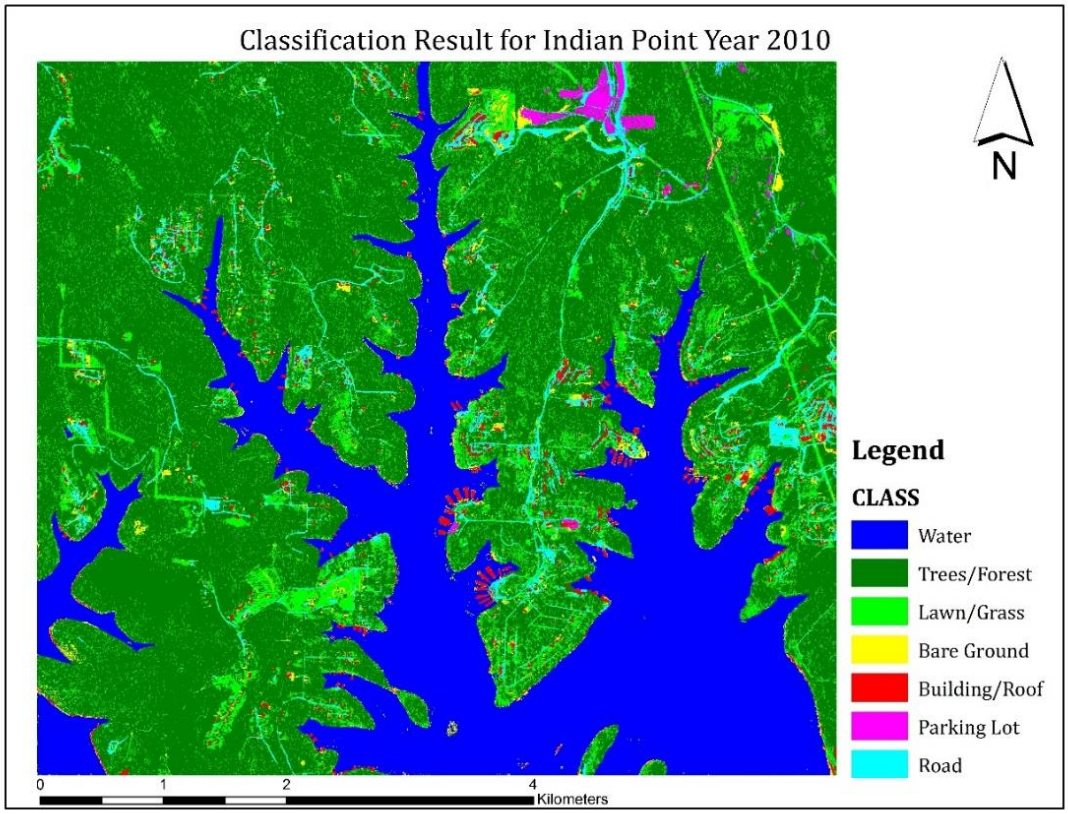
Classification Result for Indian Point Year 2010
N
Legend
CLASS
Water
Trees/Forest
Lawn/Grass
Bare Ground
Building/Roof
Parking Lot
Road
0
1
2
4
Kilometers

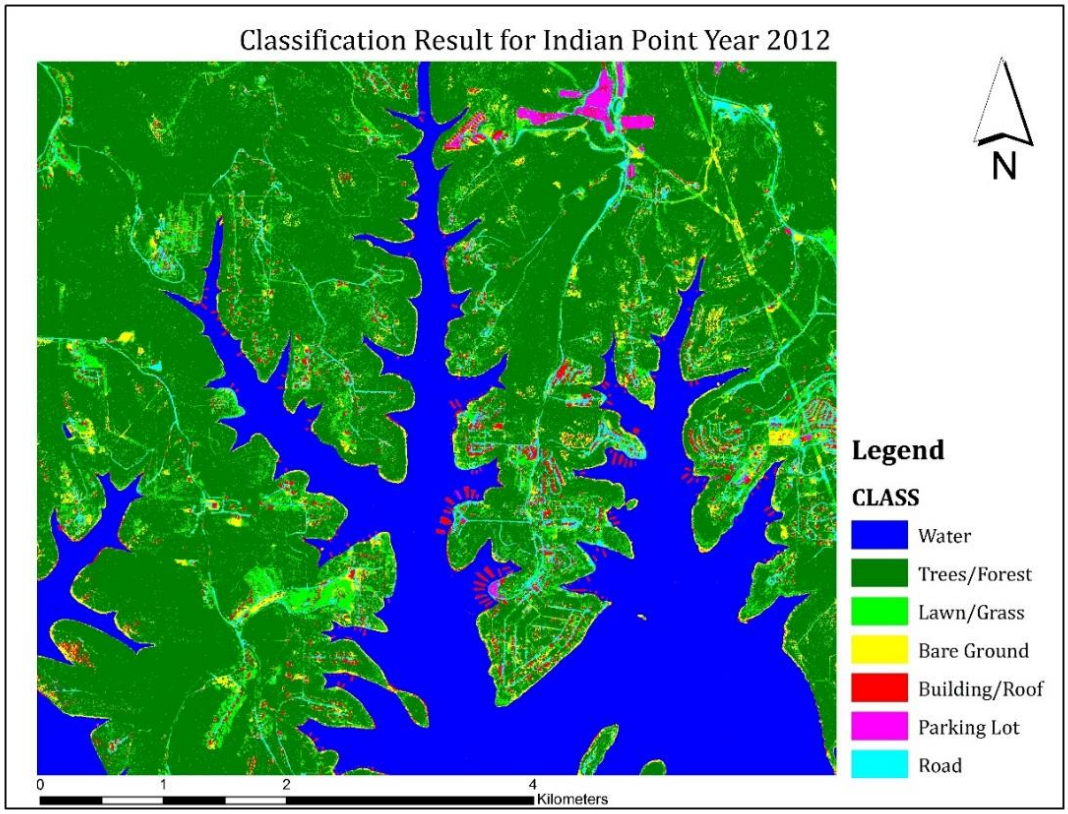
Classification Result for Indian Point Year 2012
N
Legend
CLASS
Water
Trees/Forest
Lawn/Grass
Bare Ground
Building/Roof
Parking Lot
Road
0
1
2
4
Kilometers

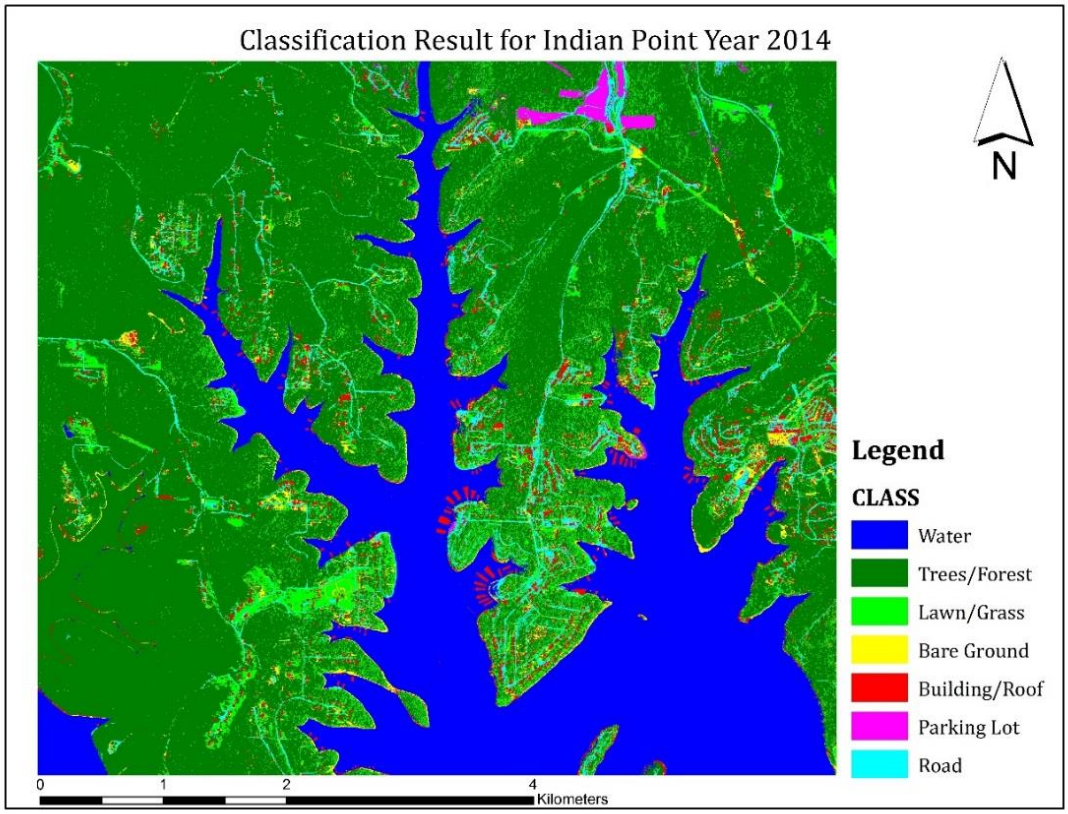
Classification Result for Indian Point Year 2014
N
Legend
CLASS
Water
Trees/Forest
Lawn/Grass
Bare Ground
Building/Roof
Parking Lot
Road
0
1
2
4
Kilometers